Title Page

Classification: Biological Sciences

Title: Plant richness, turnover and evolutionary diversity track gradients of stability and ecological opportunity in a megadiversity centre

Authors: Jonathan F. Colville[a,b,1], Colin M. Beale[c], Félix Forest[d], Res Altwegg[b,e], Brian Huntley[f], Richard M. Cowling[g,1]

Author Affiliation:

[a,1]Jonathan F. Colville: Kirstenbosch Research Centre, South African National Biodiversity Institute, Newlands, Cape Town, 7735, South Africa. ORCID identifier: https://orcid.org/0000-0003-2176-3077.

[b]Statistics in Ecology, Environment and Conservation, Department of Statistical Sciences, University of Cape Town, Rondebosch, 7701, South Africa.

[c]Colin M. Beale: Department of Biology, University of York, Heslington, York, YO10 5DD, UK. ORCID identifier: https://orcid.org/0000-0002-2960-5666.

[d]Félix Forest: Royal Botanic Gardens, Kew, Richmond, Surrey TW9 3DS, UK. ORCID identifier: https://orcid.org/0000-0002-2004-433X.

[b]Res Altwegg: South Africa and Statistics in Ecology, Environment and Conservation, Department of Statistical Sciences, University of Cape Town, Rondebosch, 7701, South Africa. ORCID identifier: 0000-0002-4083-6561.

[e]African Climate and Development Initiative, University of Cape Town, Rondebosch 7701 Cape Town, South Africa.

[f]Brian Huntley: Department of Biosciences, Durham University, South Road, Durham DH1 3LE, UK. ORCID identifier: http://orcid.org/0000-0002-3926-2257.

[g,1]Richard M. Cowling: African Centre for Coastal Palaeoscience, PO Box 77000, Nelson Mandela Metropolitan University, Port Elizabeth 6031, South Africa. ORCID identifier: 0000-0003-3514-2685.

Corresponding Author:

[1]Richard M. Cowling, Centre for Coastal Palaeoscience, PO Box 77000, Nelson Mandela Metropolitan University, Port Elizabeth 6031, South Africa; Tel.: +27 41 504 1111; Email: rmc@kingsley.co.za.

Keywords: Cape Floristic Region, longitudinal gradient, beta diversity, phylogenetic diversity, spatial models.

Abstract:

Research on global patterns of diversity has been dominated by studies seeking explanations for the equator-to-poles decline in richness of most groups of organisms, namely the latitudinal diversity gradient. A problem with this gradient is that it conflates two key explanations, namely biome stability (age and area) and productivity (ecological opportunity). Investigating longitudinal gradients in diversity can overcome this problem. Here we investigate a longitudinal gradient in plant diversity in the megadiverse Cape Floristic Region (CFR). We test predictions of the age and area and ecological opportunity hypotheses using metrics for both taxonomic and phylogenetic diversity and turnover. Our plant data set includes modelled occurrences for 4,813 species and dated molecular phylogenies for 21 clades endemic to the CFR. Climate and biome stability were quantified over the past 140 000 years for testing the age and area hypothesis, and measures of topographic diversity, rainfall seasonality and productivity were used to test the ecological opportunity hypothesis. Results from our spatial regression models showed biome stability, rainfall seasonality and topographic heterogeneity were the strongest predictors of taxonomic diversity. Biome stability alone was the strongest predictor of all diversity metrics, and productivity played only a marginal role. We argue that age and area in conjunction with non-productivity-based measures of ecological opportunity provide a robust explanation of the CFR's longitudinal diversity gradient. We suggest that this model may also be a general explanation for global diversity patterns, unconstrained as it is by the collinearities underpinning the latitudinal diversity gradient.

Significance Statement:

What explains global patterns of diversity – environmental history or ecology? Most studies have focussed on latitudinal gradients – the decline of diversity from the tropics to the poles. A problem with this gradient is that it conflates predictions of historical and ecological hypotheses: The productive tropics have also experienced high Cenozoic biome stability. Longitudinal diversity gradients can overcome this constraint. We use a longitudinal plant diversity gradient in the megadiverse Cape Floristic Region to model species and evolutionary diversity in terms of Pleistocene climate stability and ecological heterogeneity. We find that biome stability is the strongest

predictor for all diversity measures, and argue that stability, in conjunction with measures of ecological opportunity – other than productivity – provide a general explanation for global diversity patterns.

Author contributions: R.M.C., J.F.C., and F.F. designed research; R.M.C., J.F.C., C.B., and F.F. performed research; C.B., J.F.C., F.F., R.A. and B.H. analyzed data; R.M.C., J.F.C., F.F, and C.B. wrote the paper; and R.A., and B.H. revised the paper.

Text

Introduction

The roles of contemporary ecological factors vs. Cenozoic environmental stability in determining large-scale biodiversity patterns continues to generate lively debate (1–7). Research on this topic has been dominated by studies of the latitudinal decline in richness towards the poles of most taxa. The many hypotheses invoked to explain the latitudinal gradient have been elegantly distilled by Schluter (5) into two – one mainly ecological (ecological opportunity), and the other historical (age and area). The former argues that diversity patterns are underpinned by differences in ecological opportunity associated with gradients in habitat heterogeneity, productivity and the intensity of biotic interactions, all of which influence the length of niche axes: this hypothesis predicts a positive relationship between diversity and speciation rate. The age and area hypothesis posits that high diversity is a consequence of areas – sufficiently large to support viable populations of the focal taxa - having high environmental stability over evolutionary time scales, which reduces extinction rates, and results in the accumulation of species, both in old lineages and more recent radiations (2, 5, 7). Area and stability combine to increase rates of speciation and reduce rates of extinction. Large areas, being more heterogeneous, provide longer niche axes than small areas and offer more opportunities for speciation and reduced risks of extinction and overall will affect the total number of species (8–10). Environmental stability promotes high speciation rates owing to increased opportunities for niche differentiation in stable selective mosaics, but also ensures lower rates of extinction, and will affect the total number of species and their spatial arrangement (11–13). Although these two hypotheses have primarily been tested against species richness patterns, the recent increase and availability of regional species and phylogenetic datasets has enabled the testing of predictions for other diversity metrics, such as beta and phylogenetic diversity, which are central to our understanding of global diversity patterns (7, 14–18).

The age and area hypothesis predicts that biotas would have high beta diversity (changes in species composition along ecological gradients) owing to the accumulation of habitat specialists associated with both early- and later-diverging lineages. In this case, spatial turnover (species replacement),

rather than species loss (nestedness), should prevail as the driver of beta diversity (17, 19, 20) (Fig. 1A, B). The ecological opportunity hypothesis predicts the same patterns, but for a different reason: richness accumulates in areas of high ecological opportunity that foster rapid, ecological speciation in numerous clades (Fig. 1A, C). Beta diversity is largely driven by recently evolved species that have subdivided the long niche axes characteristic of high-opportunity regions. Spatial turnover should be high in areas of high ecological opportunity and high stability, allowing for the evolution of numerous range-restricted, habitat-specialist species, whereas areas of high ecological opportunity and low stability should have higher nestedness due to recolonization of empty niches after events of instability (19).

The two hypotheses make different predictions for phylogenetic diversity-based metrics. For equivalent species richness, the age and area hypothesis predicts high phylogenetic diversity, owing to the preservation of older lineages, which are widely dispersed on phylogenetic trees (Fig. 1B), whereas ecological opportunity predicts lower phylogenetic diversity owing to the preponderance of younger, recently evolved species swarms, which are mostly clustered on phylogenetic trees (Fig. 1C) (2, 7, 16, 21–23). Phylogenetic beta diversity, which measures phylogenetic turnover (i.e. turnover in branch length) (24), will vary depending on the proportion of range-restricted species present in a given area and their distribution within the phylogenetic tree (i.e. the phylogenetic distance separating them). For areas with similar species richness, phylogenetic beta diversity is predicted to be similar under the age and area hypothesis and the ecological opportunity hypothesis (15, 17, 20), although driven by different phylogenetic patterns, i.e. fewer deeper branches for the former (Fig. 1B) and many shallower branches for the latter (Fig. 1C). However, one would expect a larger proportion of widespread taxa to be present under the age and area hypothesis because of the longer time for range expansion to occur (Fig. 1B). Environmental stability fosters the large-scale preservation of clades (i.e. low extinction (Fig. 1A, B)), whereas in regions of high ecological opportunity, high diversification rates produce fewer, but more species-rich, phylogenetic groups (Fig. 1C, D) (1, 5, 7, 21–23).

123 The two hypotheses, however, are not necessarily mutually exclusive (5). A system where both
124 hypotheses have traction (i.e. a stable biome with high ecologically heterogeneity) would show high
125 beta diversity, and both high phylogenetic diversity and phylogenetic beta diversity, a consequence of
126 high speciation and low extinction rates (Fig. 1A). In this scenario, phylogenetic beta diversity can
127 also be low if most narrow-ranged species are recently-evolved (Fig. 1A(1)). On the other hand, a
128 stable biome with an ecologically homogeneous environment, and an unstable biome with an
129 ecologically heterogeneous environment, would both have high phylogenetic diversity, but it would
130 be over-dispersed in the former (i.e. principally formed of isolated lineages) (Fig. 1B) and clustered in
131 the latter (i.e. generally comprising fewer, but more speciose lineages) (Fig. 1C). Likewise, under
132 these two scenarios phylogenetic beta diversity would be high, although higher in the first case, driven
133 principally by deep branches (Fig. 1B), than in the second case, which will be driven mostly by
134 shallower branches (Fig. 1C).

135 The age and area and ecological opportunity hypotheses have seldom been tested simultaneously and
136 never for a diversity gradient within an extratropical megadiversity centre; most research has focused
137 on the latitudinal gradient, which conflates the predictions of historical and ecological hypotheses:
138 The productive tropical rainforest biomes, which offer high opportunities for ecological speciation
139 (e.g. epiphytes in tall, multi-layered forests) (4, 25, 26), have also experienced the highest stability
140 throughout the Cenozoic (2, 5, 27, 28). This problem can be overcome by researching diversity
141 gradients where environmental stability and ecological heterogeneity are uncoupled, as occurs along
142 many longitudinal diversity gradients. Examples include comparisons of diversity in temperate
143 biomes of south-eastern North America and eastern Asia (3, 29), between Europe and eastern
144 Asia/North America (30), and among the Mediterranean-climate regions across the globe (13). These
145 studies conclude that historical events and biogeographic idiosyncrasies, play a more important role in
146 explaining diversity than ecological factors associated with contemporary environments. However,
147 the world's most diverse regions, the mountainous areas of the tropical Asia and the Neotropics (1, 5,
148 7, 31), combine the environmental features predicted by both the age and area and the ecological
149 opportunity hypotheses to be associated with megadiversity.

The Cape Floristic Region (CFR), a Mediterranean-climate region, provides an excellent opportunity to investigate simultaneously the ecological and historical drivers of diversity (32). Firstly, the CFR flora is the richest extratropical flora in the world, comprising 9,383 species (68% endemic) in just 90,760 km^2. Secondly, the CFR flora is well-known taxonomically, spatially and phylogenetically. Thirdly, biological heterogeneity is relatively homogeneous throughout the region; the diversity and structure of plant communities are relatively similar for analogous landscapes throughout the CFR. Fourthly, the region shows a pronounced longitudinal gradient in regional-scale (1 – 10,000 km^2) diversity: The numbers per unit area of taxa associated with clades endemic to the CFR, as well as regional scale richness of entire floras, decline markedly in a longitudinal pattern, from south-west to south-east (32). Fifthly, longitudinal gradients of Pleistocene climatic and biome stability are evident across the CFR, with more stable climates in the west where Mediterranean climates persisted over much of the region, and less stable climates in the east where the CFR flora was replaced at times by a subtropical flora (33–35).

Here, we use the longitudinal plant diversity gradient in the CFR to test the predictions of the age and area, and ecological opportunity hypotheses to explain the longitudinal plant diversity gradient in the CFR by modelling several key diversity metrics, incorporating both species richness and evolutionary history, in relation to variables reflecting ecological and historical phenomena. Our analysis was conducted at the regional scale; our mapping unit is a two-minute grid cell (ca. 12 km^2), sufficiently large to include, in all parts of the CFR, substantial environmental gradients and several floristically distinct plant communities. Since our focus is on the evolution of CFR plant diversity, we included in our analysis only species associated with “Cape clades”, groups largely endemic to the CFR and which have their diversity centred within the region (36). Our comprehensive data set includes modelled occurrences across 8,347 two-minute grid cells for 4,813 species (~51% of total CFR species) and dated molecular phylogenies for 21 Cape clades. Patterns of Cape clade species richness are strongly correlated with overall CFR plant richness (See SI Appendix, Fig. S1) and we therefore consider them reflective of taxonomic patterns for the entire flora. We used measures of topographical heterogeneity, productivity (evapotranspiration) and rainfall seasonality as surrogates for ecological

opportunity (4, 6, 25, 37). For historical measures, climatic and biome stability were assessed using an ensemble of general circulation model experiments to calculate climatic variability and biome persistence over the last 140ky (35). This time span is appropriate for our study since many Cape clades have speciated massively during the Pleistocene (38); almost half (48.6%) of all divergence events in the current study took place in the last 2 Ma.

If the ecological opportunity hypothesis explains the CFR's species and evolutionary diversity gradients, we would expect significant positive relationships between richness, and both topographical heterogeneity and productivity, and a negative relationship between richness and rainfall seasonality (more seasonal environments precipitation becomes limiting in different seasons (i.e. precipitation only during the cool-season vs precipitation only during the warm-season) whereas less seasonal environments provide greater opportunities for niche specialization to warm- and cool-season precipitation) (32). We also expect similar relationships for beta diversity because rapid, ecological speciation should result in high spatial turnover of ecological specialists along habitat gradients. For evolutionary diversity, we expect richness hotspots to be correlated with low phylogenetic diversity per species (made up of fewer, but more speciose lineages) and relatively low phylogenetic beta diversity, owing to the predominance of recently radiating clades likely comprising range-restricted species. On the other hand, for the age and area hypothesis, we expect that richness, the spatial turnover component of beta diversity, and phylogenetic diversity all to be associated with areas of high climatic and biome stability, owing to the preservation of clades, a consequence of low extinction rates. For the same reason, phylogenetic beta diversity is more likely to be positively associated with climate and biome stability because of the prevalence of deeper branches, despite species being also more likely to exhibit wider distributions. We also predict that in regions with stable biomes and climates, and with ecologically heterogeneous landscapes, both hypothesised mechanisms will have influenced diversity patterns.

Results

Ecological and stability predictors

The spatial patterns for the five covariates used to test our predictions are shown in Fig. 2. Two nodes of high Late Pleistocene climate stability were identified, one in the west and a less pronounced one in the east CFR (Fig. 2A). However, a clear west–east gradient of biome stability was retrieved (Fig. 2B). The node of high climate stability in the east does not translate into high biome stability since eastern climates are currently marginal for Cape vegetation (32, 34) so that even small climatic shifts can cause biome replacement; thus, biome persistence was lower the eastern CFR. There is little evidence of a topographic heterogeneity gradient across the CFR; areas of high and low values are evenly spread across the region (Fig. 2C). Productivity was highest in the south-eastern and south-western CFR, and medium to low in the central and interior regions (Fig. 2D). A strong west–east seasonality gradient exists (Fig. 2E), with the west showing predominance of a winter seasonal moisture regime (See SI Appendix, Fig S1), whereas precipitation seasonality was less pronounced in the south-west, and low in the east where rainfall occurs throughout the year.

Species and evolutionary diversity patterns

The spatial patterns across the region for species and evolutionary diversity of CFR-centred plant clades are shown in Fig. 3. We recovered a marked west–east gradient in species richness across the southern CFR with highest concentrations of species in the southwest (> 380 species per grid cell) (Fig. 3A). Species richness declined eastwards into the year-round rainfall region (See SI Appendix, Fig. S2) where we recorded 65-100 species per grid cell. Total taxonomic beta diversity showed consistently high values (~0.65) across almost the entire CFR (Fig.3B) and was predominantly the result of species turnover (See SI Appendix, Fig. S3A & Fig. S3B). Nodes of high beta diversity were associated with lower mountain slopes and adjacent lowlands, areas of rapid transition of the CFR's major vegetation types, namely fynbos, renosterveld and succulent karoo (39).

Highest values of phylogenetic diversity were concentrated in the south-western CFR (Fig. 3C) and were broadly concordant with the patterns of species richness. Residuals of phylogenetic diversity over species richness showed a clear concentration of positive residuals in the eastern CFR (Fig. 3E), indicating that phylogenetic diversity is generally over-dispersed in the east and more clustered in the west. High values of phylogenetic-beta diversity were somewhat patchily distributed across the CFR

(Fig. 3D) but showed an obverse pattern to phylogenetic diversity; the south-western CFR had comparatively low phylogenetic beta diversity, most likely caused by a concentration of closely related and narrow ranged endemics (40) (as in Fig. 1A, scenario 1). Positive residuals of phylogenetic beta diversity over taxonomic beta diversity were mostly concentrated in northern parts of the CFR (Fig. 3F), where high phylogenetic beta diversity occurs without high taxonomic beta diversity (Fig. 3B). Areas of high positive residuals indicate high phylogenetic beta diversity associated with turnover of deeper branches on the phylogenetic tree (as in Fig. 1A, scenario 2). This suggests that these areas hold a high proportion (but a low absolute number) of small-ranged species belonging to older clades.

Spatial regression models

A separate full model including all covariates was run for each of the four metrics of diversity, removing one covariate at a time, and covariate support was assessed using credible intervals and wAIC statistics (*Materials and Methods;* Table 1; See SI Appendix, Table S1). The direction of the relationship and the strength of the effect the covariate has on a diversity variable are summarized in Table 1 and Fig. 4 (full details in SI Appendix, Fig. S4, Table S1, S2).

For species richness we found strong evidence (support both from credible intervals and wAIC statistics) for a positive relationship with both biome stability and topographic heterogeneity, and a negative relationship with seasonality (areas with moderate seasonality in the south-western and southern CFR generally had higher richness whereas high-seasonality areas in the north-western CFR were relatively species poor, as were the areas of lowest seasonality in the east) (Fig. 2). Species richness showed marginal positive relationships with productivity and climatic stability.

Before controlling for species richness, we found that ecological covariates were the best predictors for taxonomic beta diversity; however, the direction of these relationships did not all match the direction of our predictions (Fig. 1). We recorded a negative effect with topographic heterogeneity and productivity, and a positive effect with seasonality; topographic heterogeneity and seasonality also received support from wAIC statistics. Controlling for species richness altered these relationships

and only topographic heterogeneity (negative relationship) was retained as a marginally significant ecological predictor, whereas both historical stability predictors showed well-supported positive effects. Biome stability received additional support from wAIC statistics and therefore emerged as the most robust predictor of taxonomic beta diversity.

For metrics of evolutionary diversity, we found a similar pattern for phylogenetic diversity to that observed for species richness, with all covariates having a strong effect (Table 1). Other than seasonality, which was negatively related to phylogenetic diversity, all covariates showed positive relationships with this metric. As was the case for species richness, models excluding climatic stability or productivity received more support from wAIC statistics than the full model, indicating that the positive effects of biome stability and topographic heterogeneity, and the negative effects of seasonality, are best at predicting phylogenetic diversity. However, when controlling for species richness, almost all the strong effects of covariates disappeared, except for the positive relationship with biome stability.

For phylogenetic beta diversity, we found well-supported negative relationships with all covariates, except for seasonality. Seasonality showed a well-supported positive relationship, with areas of high seasonality (the strongly winter-rainfall, north-western CFR) having high phylogenetic beta diversity. After accounting for species richness, the model retained a well-supported negative relationship between phylogenetic beta diversity and biome stability and productivity. Climatic stability offered marginal support for a negative relationship with phylogenetic beta diversity, while seasonality retained marginal support for a positive relationship. Phylogenetic beta diversity, therefore, appears highest in less stable and low-productivity environments such as the northern fringes of the eastern CFR.

Overall, results from our spatial regression models support our predictions of greater species and phylogenetic diversity (Fig. 1A) and lower phylogenetic beta diversity (Fig.1A, scenario 1) associated with the areas of high biome stability, namely the south-western CFR. These areas support the highest numbers of taxa, many of which are range-restricted and recently-diversified (See SI Appendix, Fig.

S3, Table S3). We also found well-supported evidence consistent with the prediction that the turnover component of taxonomic beta diversity would be positively related to biome stability (Fig. 1A, B). We found mostly marginal support for the role of ecological predictors in patterns of diversity, and the directions of the individual diversity-covariate relationships did not always follow expected predictions. Although topographical heterogeneity showed a strong positive relationship with species richness (Fig. 1A), it had a strong negative relationship with beta diversity, contrary to our predictions (Fig. 1A, C). Our prediction that topographical heterogeneity would have a strong, positive relationship with evolutionary diversity metrics (Fig. 1A, C), was also rejected. Our prediction that productivity would be positively related to species-richness was only marginally supported, and we retrieved little support for our prediction of a positive relationship between phylogenetic diversity and productivity (Fig. 1A, C). We also did not find support for the prediction that taxonomic beta diversity would be positively related to productivity; instead we found some support for a negative relationship. Contrary to our predictions (Fig.1A, scenario 2), phylogenetic beta diversity was negatively associated with climatic and biome stability, and productivity.

Discussion

As an extratropical centre of plant megadiversity, the diversity of the CFR has puzzled evolutionary biologists for decades. A relatively recent model for predicting global plant diversity patterns, which used measures of productivity and topographic heterogeneity as explanatory variables, while explaining diversity patterns for other bioregions, predicted half the observed species richness of the CFR (37). Here we show that biome stability (age and area), in combination with low seasonality and high topographic heterogeneity (ecological opportunity), were the best predictors of taxonomic plant richness in the CFR (Fig. 1A). Importantly, productivity, widely invoked as a key driver of global patterns of richness (4, 25, 37), played only a marginal role in explaining these patterns (see also 7). We recognize, however, that we have presented a set of verbal predictions that may not fully capture how different processes map to patterns. Further testing of our predictions by simulation with a wider range of parameters would help to confirm the importance of biome stability in shaping regional diversity patterns.

Our results go to the heart of one of the most enduring patterns in ecology and evolution: areas of high productivity (such as the humid tropics) are repositories of large amounts of diversity. While the CFR has long been seen as an exception to this rule (13, 32), ours is the first study to demonstrate this analytically. The relationship between energy and diversity is largely the historical legacy of a warm and wet world during the Cenozoic (2, 5, 7), which was disrupted since the mid-Miocene by progressive aridification and cooling. Tropical areas may well be diverse not primarily because of high water-energy regimes, but because of age and area; their biotas have persisted in vast equatorial regions for the past 60 My, resulting in a far greater accumulation of species than in the younger temperate and arctic zones (1, 5, 6, 41). In this sense the CFR is not an exception but a robust example of a general model for explaining regional-scale taxonomic diversity gradients: richness patterns can be best predicted by measures of Cenozoic environmental stability.

Other important metrics of diversity also appear best explained by measures of stability, with positive correlations retrieved for all but one diversity metric, namely phylogenetic beta diversity. High values of species turnover (~ 60% changes in species composition) were recorded throughout the CFR and showed a strong positive correlation with biome stability. Contrary to our predictions (e.g. Fig. 1A), greater ecological opportunity did not necessarily equate to higher values of species turnover. This pattern is likely a consequence of biome stability allowing the persistence in and generation of habitat specialists (greater niche filling) in the south-western CFR, from both young and old lineages. The pattern cannot be attributed to topographical heterogeneity *per se* since this is essentially invariant across the CFR (32, 42). The low ratio of species loss (the nestedness component of beta diversity) in the less stable areas of the eastern CFR is surprising considering the findings by other studies where high nestedness was associated with areas experiencing climatic instability (e.g. see 17, 21, 43, 44). However, by focusing only on Cape clades , which tend to be habitat specialists, we do not fully capture the many habitat generalists associated with widespread clades that are best represented in the eastern CFR (33, 39), and which may contribute more to nestedness.

Phylogenetic diversity in the CFR shows patterns similar to species richness, with a concentration of high values in the western part of the region. Our results confirm that overall, phylogenetic diversity is more evenly distributed in the phylogenetic tree, and generally on longer branches (i.e. overdispersed), in the eastern CFR (45, 46). Our finding of a strong positive relationship of phylogenetic diversity with biome stability (Table 1) supports this pattern, which can be explained by the presence in the western part of the CFR of a high number of closely related taxa that accumulated over time in a relatively stable environment (see (45)). The strong relationship of phylogenetic diversity with biome stability may suggest high speciation rates coupled to lower extinction rates for the south-western CFR (e.g. (42); Fig 1A). However, owing to the high incidence range-restricted taxa in the western CFR (40, 42), extinction rates may likely be high (47). On the other hand, the eastern CFR has experienced greater biome instability, leading to limited speciation and increased extinction compared to the western part of the region, as exemplified by the presence of fewer species from more disparate lineages positioned on long branches in the phylogenetic tree (e.g. (45); Fig. 1D). Importantly, paleoecological data modelling studies suggest more stable biomes and environments in the western than eastern CFR during the Late Pleistocene; during glacial periods CFR biomes persisted or even expanded in the west, in the east, large areas were replaced by subtropical grassland (e.g. (44, 48–50)).

The phylogenetic beta diversity patterns revealed here are somewhat more difficult to explain and need to be considered in parallel with taxonomic beta diversity (24). High levels of phylogenetic beta diversity and positive residuals (i.e. excess phylogenetic beta diversity above and beyond that expected from taxonomic beta diversity) were found mostly in the north of the CFR, with low levels of phylogenetic beta diversity (and negative residuals) concentrated in the south-west corner of the region. This suggests that these areas hold a high proportion (but a low absolute number) of small ranged species (40, 42) belonging to older clades (Fig. 1A, scenario 2). However, some species near the northern boundaries of the CFR may be present in only a few localities within the CFR but have a much wider range extending outside of the region. This would bias the results towards higher

phylogenetic beta diversity values in the northern part of the CFR because these potentially wider ranges would not be accounted for in the present calculations. On the other hand, the coastal regions of the CFR are mostly characterised by negative residuals and high taxonomic beta diversity (Fig. 3B, E), which indicates the presence of a high proportion of range-restricted species, mostly from recently diversified clades (Fig. 1A, scenario 1).

Using a region of extraordinarily high plant richness and endemism we conclude that age and area best explains large-scale patterns of plant diversity. We further argue that far from being the exception, the CFR model suggests that environmental stability may be the primary predictor of plant megadiversity. This explanation, retrieved for a longitudinal gradient, is equally applicable to the intensively researched latitudinal diversity gradient (1, 5, 21, 51). Our use of a longitudinal gradient of diversity is important in that it allowed us to explore predictors of regional-scale diversity not necessarily concordant with gradients of productivity. Given sufficient biome stability in combination with high ecological opportunity, we see no reason why megadiversity should not evolve in low-production bioregions. An illustrative example is the extraordinarily high biodiversity of South Africa's winter-rainfall desert – the Succulent Karoo – which, like the adjacent CFR, enjoyed a relatively stable Pleistocene climate (52).

Material & Methods

Cape plant database

We built a plant species distributional database for South African angiosperms incorporating data from national plant atlas and citizen science projects, and databased herbarium specimens (53–56). The final database comprised 19,622 taxa (ca 96% of South African taxa) (57) and just over1.8 million point locality records. In order to account for the inherent biases in such presence-only or "atlas-type" data, we employed a geospatial modelling technique (58) to interpolate the distribution records for each plant species and to calculate a continuous probability of occurrence surface for each species at a two minute grid cell scale (~ 12km^2), with an associated measure of uncertainty. We

followed the same modelling procedures ("Spatial Model 1") described in detail by (58) and using code provided in Spatial Model 1 that built on earlier models by (59). For each species, we built a model at two minute resolution combining point pattern analysis methods with environmental niche information, to account for ecological similarity, inferred observer effort and geographical distance. Briefly, this process involved two stages, each consisting of a number of separate steps. The first stage involved selecting a sample of non-focal species records to act as pseudo-absences (reflecting the pattern of observation in the dataset), and the second stage involved interpolating distributions based on presence and pseudo-absence records. In slightly more detail, the first stage required (1) mapping all records of the focal species and generating a kernel density estimate for records of this species; (2) identifying all records of all other plant species (not just representatives of Cape Clades) > 100m from records of the focal species and generating similar kernel density estimates; (3) computation of the difference in density estimates between focal and non-focal species (an approximate index of the probability of encountering the focal species); (4) computation of an environmental envelope within a principal component analysis of rainfall (mean annual rainfall and rainfall season) (60) and temperature variables (mean winter and mean summer temperature) (60) and soil covariates (61) (means taken from aggregating original soil data resolution of ca. $1km^2$ to our ca. $12km^2$ grid cell size; soil properties: % calcium carbonate, % clay, % silt, % sand; and pH); (5) computing the environmental distance between all two minute raster cells and the centroid of the environmental envelope occupied by the focal species; and (6) sampling records of the non-focal species using the environmental distance and geographic probability of encountering the focal species to bias selection towards locations where absence was most likely. With pseudo-absence records selected, the second stage of analysis involved regression kriging of the presence / absence points onto the two minute raster surface, using the rainfall, temperature and soil covariates. For species recorded from <5 locations in the database, we were unable accurately to interpolate distribution and simply generated a raster map with presence (1) and assumed absence (0) directly from the recorded data. We sought to verify distributions for well-known species, sending maps to colleagues with detailed knowledge of the species groups concerned and asking for expert opinion on the map quality. Our estimated species richness patterns were consistent with expert opinion. Once the surfaces for probability of occurrence

of all species were calculated, we then selected only those species associated with pre-defined Cape clades (following the criteria of (36): CFR origin and > 50% of species native to the CFR) and for which phylogenetic data were available (Table S3). Finally, the calculated probability of occurrence surfaces for all Cape clade species was clipped to the extent of the CFR as defined by (62). Our final Cape clade database consisted of modelled occurrences across 8,347 two-minute grid cells for 4,813 taxa (51% of total CFR species (63)). These probabilities of occurrence surfaces were used in all our metrics of contemporary and evolutionary diversity. All data analyses and geospatial modelling were undertaken in R (64) using packages *spatstat* (65), *sp* (66, 67), *rgdal* (68) and *gstat* (69).

Taxonomic plant diversity

We calculated two measures of taxonomic species diversity: species richness and beta diversity. Species richness was calculated for each grid cell as the summed probability surfaces for all our Cape clade species. Three different measures of beta diversity were calculated using the indices presented by (19): Sorenson's beta-diversity ($ß_{sor} = b + c /(2a + b + c)$) and its two component parts of Simpson's spatial turnover $ß_{sim} = \min(b,c)/[a + \min(b,c)]$ and nestedness $ß_{nes} = ß_{sor} - ß_{sim}$. Variable *a* is the number of species common to a focal and neighbour grid cell, *b* is the number of species that occur only in the focal grid cell, and *c* is the number of species that occur only in the adjacent cell. In each case we computed *a*, *b* and *c* based on probabilities of presence: *a* was simply the sum of the probability of presence of all species; *b,* the sum of the product of the probabilities that a species was present in the focal cell, but absent in a neighbour; and *c*, the sum of the product of the probabilities that a species was absent in the focal cell, but present in a neighbour. Using interpolated species distributions offered advantages over and above raw presence-only data, as our beta diversity indices were not overly biased by gaps in the data (i.e. false absences). Calculated beta diversity for each grid cell represented the mean value of probabilities between the focal cell and all its neighbours (maximum of eight). We specifically partitioned beta diversity into its two component parts across the CFR, as the processes associated with species loss and gain (nestedness) and replacement (turnover) can be fundamentally different and can offer contrasting insights into the generation of diversity (17, 19, 43).

446 **Phylogenetic plant diversity**

447 Phylogenetic diversity metrics were computed for 21 Cape clades for which molecular data were
448 available (See SI Appendix, Table S3). Phylogenetic trees were compiled from one of three data
449 sources: 1) trees acquired directly from the publication or provided by the authors; 2) matrices
450 obtained from the publication or from the authors; and 3) sequence data downloaded from GenBank.
451 Trees acquired directly from their published source were made ultrametric using the function chronos
452 (70) as implemented in the R package APE (71), which implements the penalized likelihood method
453 (72). The "correlated" model of substitution rate variation among branches was applied and the root
454 of the tree was assigned a value of 1.0. If an ultrametric tree was obtained directly from the original
455 publication, it was standardised so that its root was given a value of 1.0. For cases for which either
456 matrices or sequence data were obtained, the software RAxML (v. 8.2.8), as implemented on the
457 Cipres portal (www.phylo.org), was used to reconstruct a phylogenetic tree under the maximum
458 likelihood (ML) criterion, with 1,000 rapid bootstrap replicates followed by the search of the best ML
459 tree; the GTRCAT model was used and all other parameters were set up with their default settings.
460 DNA sequence data were retrieved from GenBank using Geneious (version 7.1.2) (73) and aligned
461 using the MUSCLE (74) algorithm. The approach used for each Cape clade is described in Table S3.

462 The 21 individual species-level Cape clade trees were grafted onto a previously published genus-level
463 phylogeny of the Cape flora (45). This approach was favoured for several reasons. First, accurately
464 calibrating phylogenetic trees from Cape groups is particularly difficult due to the limited information
465 available in the fossil record for the vast majority of these clades (e.g. (36)). Second, the comparison
466 of phylogenetic diversity metrics between clades would be invalid if all clades were in effect assigned
467 the same age, as performed here (i.e. all root ages assigned a value of 1.0), which they are evidently
468 not (e.g. (38, 49, 75)). Third, embedding all 21 Cape clades in a flora-wide tree allows us to compile
469 overall phylogenetic diversity metrics for all clades and account for their deep history, which is
470 particularly important in the case of phylogenetic beta diversity because the age of a group will
471 significantly affect turnover in branch lengths (i.e. shallow vs deep branches).

The function *paste.tree* from the R package *phytools* (76) was used to graft the individual trees onto the Cape flora genus-level tree. For clades comprising more than one genus (e.g. Bruniaceae, Podalyrieae, Restionaceae), all genera except one (randomly selected) were first pruned so that all 21 clades are represented by only one branch in the Cape flora tree. For each clade, the crown node was grafted in the middle of the corresponding branch in the Cape flora tree. Phylogenetic diversity and phylogenetic beta diversity metrics were calculated with the resulting Cape flora genus-level tree comprising the grafted Cape clades, considering only the species found in the Cape clades in the calculations (i.e. the other genera included in the Cape flora tree were not considered here).

Phylogenetic diversity was calculated for each grid as the sum of all branches connecting all members of a set of taxa, including the root of the tree. Branch lengths were weighted using the same probabilistic computations used for species diversity (see above), with a terminal branch weighted by the probability of occurrence in a given cell of the species it represents, while all internal branches were weighted by the joint probability of occurrence in a given cell of all the species it subtends. Phylogenetic beta diversity was compiled using Sorenson's index, similarly to taxonomic beta diversity as described above, where variable a is the sum of the branch lengths common to a given grid cell and an adjoining grid cell, b is the sum of the branch lengths that only occur in a given grid cell, and c is the sum of the branch lengths that occur only in the adjacent cell. As for the phylogenetic diversity calculation, branch lengths were weighted using their probability of occurrence in each grid cell.

Surrogate variables for ecological opportunity

We calculated topographic heterogeneity from the Shuttle Radar Topography Mission (SRTM) digital elevation model (DEM; available from http://earthexplorer.usgs.gov/) computing the mean absolute difference in altitude between the focal pixel and its eight neighbours at the native 30m resolution (77), then calculating the median value per two minute grid cell (See SI Appendix, Fig. S5). As beta-diversity was measured at two minute resolution, we further compared this measure of topographic heterogeneity with the somewhat cruder analysis generated by first aggregating the DEM data to 2

minute resolution and computing the mean altitude, then computing roughness on this using the same algorithm. These two alternative surfaces were correlated at r = 0.632, so we used the first in all analyses (See SI Appendix, Fig. S5). Seasonality was calculated using a measure of rainfall concentration (ranging between 0% for zero seasonality to 100% for all rainfall in a single month) (60). We used as a measure of productivity, annual actual evapotranspiration obtained from satellite data (MOD16A2 Version 6 Evapotranspiration/Latent Heat Flux product is an 8-day composite product produced at 500 metre pixel resolution (78)). Actual evapotranspiration is a measure of water-energy balance closely associated with plant productivity (4). We used 8-day values to generate an annual value (mm/a) and aggregated this to our two-minute grid taking the median value for each two-minute cell.

Surrogate variables for environmental stability

We investigated climate and biome changes over the 140ka, a period spanning two major glacial-interglacial cycles (Marine Oxygen Isotope Stages 6 to 1) (35). Results from 78 palaeoclimate experiments and a pre-industrial experiment made with a consistent configuration of the Hadley Centre unified model (79), a fully-coupled atmosphere–ocean general circulation model (80), were used to compute anomalies for monthly mean temperature, precipitation and cloudiness. Thin-plate splines fitted to these anomalies (81) were used to interpolate them to a 0·5° grid. Palaeoclimate scenarios at 0·5° grid resolution were then generated for the 78 time slices by applying the interpolated anomalies to observed recent (1961–90) values in the CRU CL 1.0 dataset (82). Nine bioclimatic variables were computed for each grid cell and time slice, including 1961–90: annual thermal sums above 0°C and 5°C; mean temperatures of the coldest and warmest months; an estimate of the annual ratio of actual to potential evapotranspiration; annual total intensity of the wet and dry season(s); and maximum wet and dry season intensity (for details see (35)). Values for each bioclimatic variable were then standardised to zero mean and unit standard deviation across all grid cells and time slices, the standardised values being used to compute Euclidean distances between all 3081 possible time-slice pairs for each grid cell. Finally, the mean of the Euclidean distances for a

grid cell was used as the metric of climatic stability, smaller values indicating greater stability. No two covariates were particularly strongly correlated (all $r < 0.6$; See SI Appendix, Fig. S6).

The relationships between the relative extents in each 0·5° grid cell of each of the nine regional biomes (39) and present climate were modelled using quantitative climatic response surfaces (79). Details of the modelling approach are given by (35). These models were used to simulate the relative extent of each biome in each grid cell for each of the 79 time slices. The frequency with which each biome dominated each grid cell (i.e. had the greatest relative extent) across time slices was counted and the biome with the highest frequency of dominance in a grid cell was identified and its frequency used as the metric of biome stability for that grid cell. After computation, we downscaled predictions to our 2-minute raster using bilinear interpolation.

Spatial regression models

To test predictions about drivers of diversity we fitted spatial regression models to each of the taxonomic and phylogenetic diversity surfaces, using covariates (topographic heterogeneity, actual evapotranspiration, rainfall seasonality, and biome and climatic stability) representing the primary hypotheses to predict diversity patterns. Specifically, we fitted intrinsic Continuous Autoregressive (iCAR (83)) models using Integrated Nested Laplace Approximation (INLA (84)) via the R-INLA package (85). iCAR models have been shown to perform well in a variety of spatial regression situations (86) and INLA provides a fast, Bayesian approach to fitting these computationally demanding models. As components of beta diversity (taxonomic and phylogenetic) and phylogenetic diversity measures are strongly influenced by local gradients in species richness (19, 45) we fitted further models to predict these variables that also included species richness as a covariate, expecting that including this covariate would remove relationships that are due primarily to drivers of species richness, rather than beta and phylogenetic diversity *per se*. We expect the models with species richness to be both more conservative and more reliable, but included models without them to facilitate understanding of the simpler relationships. As INLA provides a Bayesian approach to model fitting we assessed support for parameter estimates by identifying whether or not 95% Credible Intervals (CIs) overlapped zero. Although there appears to be potential for a degree of circularity in

our use of environmental variables to model species distributions and then relating modelled species data to environmental data in our spatial regression models, it will not necessarily do so and previous work demonstrates that covariates predicting richness can be markedly different to covariates predicting individual distributions (58). If this potential circularity was problematic, we would expect that the environmental data to outperform the other covariates, but as our results did not support this, we can be confident our results are not an artefact.

Data Availability

Plant species and phylogenetic data are available from published sources and online repositories listed in Material & Methods and Supporting Information.

Acknowledgments

J.F.C was supported by a South African National Research Foundation Research Career Advancement Fellowship (grant no. 91442). J.F.C and C.B were supported with travel funding through a British Council Researcher Links Travel Grant. R.A. was supported with funding from the South African National Research Foundation (grant no. 85802 and 119125). BH was supported by a Leverhulme Trust Research Grant (F/00 128/BI) and a Durham University Matariki Partnership Travel Grant. The authors acknowledge the Centre for High Performance Computing (CHPC), South Africa, for providing computational resources to this research project, and for the assistance of Kevin Colville. We thank John Manning, Toney Rebello and Les Powrie for their expert opinion on species distribution maps.

572 **References**

573 1. G. G. Mittelbach, *et al.*, Evolution and the latitudinal diversity gradient: Speciation, extinction
574 and biogeography. *Ecol. Lett.* **10**, 315–331 (2007).

575 2. R. E. Ricklefs, Evolutionary diversification and the origin of the diversity-environment
576 relationship. *Ecology* **87**, S3-13 (2006).

577 3. H. Qian, R. E. Ricklefs, Large-scale processes and the Asian bias in species diversity of
578 temperate plants. *Nature* **407**, 180–182 (2000).

579 4. B. A. Hawkins, *et al.*, Energy, water, and broad-scale geographic patterns of species richness.
580 *Ecology* **84**, 3105–17 (2003).

581 5. D. Schluter, Speciation, ecological opportunity, and latitude. *Am. Nat.* **187**, 1–18 (2016).

582 6. R. E. Latham, R. E. Ricklefs, Global patterns of tree species richness in moist forests: Energy-
583 diversity theory does not account for variation in species richness. *Oikos* **67**, 325 (2006).

584 7. P. V. A. Fine, Ecological and evolutionary drivers of geographic variation in species diversity.
585 *Annu. Rev. Ecol. Evol. Syst.* **46**, 369–392 (2015).

586 8. M. L. Rosenzweig, *Species diversity in space and time* (Cambridge University Press, 1995).

587 9. R. A. Pyron, J. J. Wiens, Large-scale phylogenetic analyses reveal the causes of high tropical
588 amphibian diversity. *Proc. R. Soc. B Biol. Sci.* **280** (2013).

589 10. J. B. Losos, D. Schluter, Analysis of an evolutionary species–area relationship. *Nature* **408**,
590 847–850 (2000).

591 11. S. D. Hopper, OCBIL theory: Towards an integrated understanding of the evolution, ecology
592 and conservation of biodiversity on old, climatically buffered, infertile landscapes. *Plant Soil*
593 **322**, 49–86 (2009).

594 12. N. Morueta-Holme, *et al.*, Habitat area and climate stability determine geographical variation

595 in plant species range sizes. *Ecol. Lett.* **16**, 1446–1454 (2013).

596 13. R. M. Cowling, *et al.*, Variation in plant diversity in mediterranean-climate ecosystems: The
597 role of climatic and topographical stability. *J. Biogeogr.* **42** (2015).

598 14. H. Qian, R. E. Ricklefs, A latitudinal gradient in large-scale beta diversity for vascular plants
599 in North America. *Ecol. Lett.* **10**, 737–44 (2007).

600 15. H. Qian, N. G. Swenson, J. Zhang, Phylogenetic beta diversity of angiosperms in North
601 America. *Glob. Ecol. Biogeogr.* **22**, 1152–1161 (2013).

602 16. J. C. Massante, *et al.*, Contrasting latitudinal patterns in phylogenetic diversity between woody
603 and herbaceous communities. *Sci. Rep.* **9**, 1–10 (2019).

604 17. J. N. Pinto-Ledezma, D. J. Larkin, J. Cavender-Bares, Patterns of beta diversity of vascular
605 plants and their correspondence with biome boundaries across North America. *Front. Ecol.*
606 *Evol.* **6**, 1–13 (2018).

607 18. C. Lamanna, *et al.*, Functional trait space and the latitudinal diversity gradient. *Proc. Natl.*
608 *Acad. Sci.* **111**, 13745–13750 (2014).

609 19. A. Baselga, Partitioning the turnover and nestedness components of beta diversity. *Glob. Ecol.*
610 *Biogeogr.* **19**, 134–143 (2010).

611 20. I. R. McFadden, *et al.*, Temperature shapes opposing latitudinal gradients of plant taxonomic
612 and phylogenetic β diversity. *Ecol. Lett.* **22**, 11226–1135 (2019).

613 21. P. D. Mannion, P. Upchurch, R. B. J. Benson, A. Goswami, The latitudinal biodiversity
614 gradient through deep time. *Trends Ecol. Evol.* **29**, 42–50 (2014).

615 22. H. Qian, Y. Jin, R. E. Ricklefs, Phylogenetic diversity anomaly in angiosperms between
616 eastern Asia and eastern North America. *Proc. Natl. Acad. Sci.* **114**, 11452–11457 (2017).

617 23. H. Qian, Y. Zhang, J. Zhang, X. Wang, Latitudinal gradients in phylogenetic relatedness of

618 angiosperm trees in North America. *Glob. Ecol. Biogeogr.* **22**, 1183–1191 (2013).

619 24. C. H. Graham, P. V. A. Fine, Phylogenetic beta diversity: linking ecological and evolutionary
620 processes across space in time. *Ecol. Lett.* **11**, 1265–77 (2008).

621 25. D. J. Currie, Energy and large-scale patterns of animal- and plant-species richness. *Am. Nat.*
622 **137**, 27–49 (1991).

623 26. A. R. Cirtwill, D. B. Stouffer, T. N. Romanuk, Latitudinal gradients in biotic niche breadth
624 vary across ecosystem types. *Proc. R. Soc. London B Biol. Sci.* **282** (2015).

625 27. T. van der Hammen, M. L. Absy, Amazonia during the last glacial. *Palaeogeogr.*
626 *Palaeoclimatol. Palaeoecol.* **109**, 247–261 (1994).

627 28. T. van der Hammen, H. Hooghiemstra, Neogene and Quaternary history of vegetation, climate,
628 and plant diversity in Amazonia. *Quat. Sci. Rev.* **19**, 725–742 (2000).

629 29. H. Qian, R. E. Ricklefs, P. S. White, Beta diversity of angiosperms in temperate floras of
630 eastern Asia and eastern North America. *Ecol. Lett.* **8**, 15–22 (2005).

631 30. B. Huntley, Species-richness in north-temperate zone forests. *J. Biogeogr.* **20**, 163 (1993).

632 31. C. Hughes, R. Eastwood, Island radiation on a continental scale: Exceptional rates of plant
633 diversification after uplift of the Andes. *Proc. Natl. Acad. Sci.* **103**, 10334–10339 (2006).

634 32. R. M. Cowling, P. L. Bradshaw, J. F. Colville, F. Forest, Levyns' law: explaining the evolution
635 of a remarkable longitudinal gradient in Cape plant diversity. *Trans. R. Soc. South Africa* **0**, 1–
636 18 (2017).

637 33. F. A. Engelbrecht, *et al.*, Downscaling Last Glacial Maximum climate over southern Africa.
638 *Quat. Sci. Rev.* **In press.** (2020).

639 34. M. Bar-Matthews, *et al.*, A high resolution and continuous isotopic speleothem record of
640 paleoclimate and paleoenvironment from 90 to 53 ka from Pinnacle Point on the south coast of

South Africa. *Quat. Sci. Rev.* **29**, 2131–2145 (2010).

35. B. Huntley, *et al.*, Explaining patterns of avian diversity and endemicity: Climate and biomes of southern Africa over the last 140,000 years. *J. Biogeogr.* **43**, 874–886 (2016).

36. H. P. Linder, The radiation of the Cape flora, southern Africa. *Biol. Rev. Camb. Philos. Soc.* **78**, 597–638 (2003).

37. H. Kreft, W. Jetz, Global patterns and determinants of vascular plant diversity. *Proc. Natl. Acad. Sci. U. S. A.* **104**, 5925–30 (2007).

38. H. P. Linder, Evolution of diversity: the Cape flora. *Trends Plant Sci.* **10**, 536–41 (2005).

39. L. Mucina, M. C. Rutherford, *The vegetation of South Africa, Lesotho and Swaziland.Strelitzia 19.* (South African National Biodiversity Institute, 2006).

40. P. L. Bradshaw, J. F. Colville, H. P. Linder, Optimising regionalisation techniques: Identifying centres of endemism in the extraordinarily endemic-rich cape floristic region. *PLoS One* **10** (2015).

41. R. Jansson, M. Dynesius, The Fate of clades in a world of recurrent climatic change: Milankovitch oscillations and evolution. *Annu. Rev. Ecol. Syst.* **33**, 741–777 (2002).

42. R. M. Cowling, A. T. Lombard, Heterogeneity, speciation/extinction history and climate: explaining regional plant diversity patterns in the Cape Floristic Region. *Divers. Distrib.* **8**, 163–179 (2002).

43. R. Dobrovolski, A. S. Melo, F. A. S. Cassemiro, J. A. F. Diniz-Filho, Climatic history and dispersal ability explain the relative importance of turnover and nestedness components of beta diversity. *Glob. Ecol. Biogeogr.* **21**, 191–197 (2012).

44. R. M. Cowling, A. J. Potts, G. F. Midgley, C. W. Marean, Describing a drowned ecosystem: Last Glacial Maximum vegetation reconstruction of the Palaeo-Agulhas Plain. *Quat. Sci. Rev.* **In press** (2020).

665 45. F. Forest, *et al.*, Preserving the evolutionary potential of floras in biodiversity hotspots. *Nature*
666 **445**, 757–60 (2007).

667 46. F. Forest, J. F. Colville, R. M. Cowling, "Evolutionary diversity patterns in the Cape flora of
668 South Africa" in *Phylogenetic Diversity: Applications and Challenges in Biodiversity Science*,
669 (Springer, Switzerland, 2018), pp. 167–187.

670 47. S. Buerki, *et al.*, Contrasting biogeographic and diversification patterns in two mediterranean-
671 type ecosystems. *PLoS One* **7** (2012).

672 48. C. W. Marean, *et al.*, "Stone age people in a changing South African Greater Cape Floristic
673 Region" in *Fynbos: Ecology, Evolution, and Conservation of a Megadiverse Region*, N.
674 Allsopp, J. F. Colville, G. A. Verboom, Eds. (Oxford University Press, 2014), pp. 164–199.

675 49. G. A. Verboom, H. P. Linder, V. Hoffmann, N. G. Bergh, R. M. Cowling, "Cenozoic assembly
676 of the Greater Cape flora" in *Fynbos: Ecology, Evolution, and Conservation of a Megadiverse*
677 *Region*, N. Allsopp, J. F. Colville, G. A. Verboom, Eds. (Oxford University Press, 2014), pp.
678 93–118.

679 50. K. Braun, *et al.*, A climate and environment record dating between ~444 and 41 ka from
680 Pinnacle Point (south coast, South Africa) as derived from speleothem stable isotopic
681 compositions. *Quat. Res.* **91**, 265–288 (2019).

682 51. R. E. Ricklefs, Evolutionary diversification and the origin of the diversity–environment
683 relationship. *Ecology* **87**, 3–13 (2006).

684 52. R. M. Cowling, P. G. Desmet, P. W. Rundel, K. J. Esler, Extraordinary high regional-scale
685 plant diversity in southern African arid lands: Subcontinental and global comparisons. *Divers.*
686 *Distrib.* **4**, 27–36 (1998).

687 53. , Protea Atlas Project. *Natl. Bot. Institute, Kirstenbosch* (1991).

688 54. G. Germishuizen, N. L. Meyer, Plants of southern Africa: An annotated checklist. National

689 Botanical Institute, Pretoria. *Strelitzia* **14** (2003).

690 55. , BRAHMS - SANBI herbarium specimen data from PRECIS (National Herbarium Pretoria
691 (PRE) Computerized Information System) database and additional data.

692 56. SANBI, CREW/TSP/MSB/ISEP - Threatened Plant Localities database, SANBI - CapeNature.

693 57. D. Raimondo, The Red List of South African plants - A global first. *S. Afr. J. Sci.* **107**, 1–2
694 (2011).

695 58. S. Mecenero, R. Altwegg, J. F. Colville, C. M. Beale, Roles of spatial scale and rarity on the
696 relationship between butterfly species richness and human density in South Africa. *PLoS One*
697 **10**, e0124327 (2015).

698 59. T. Hengl, H. Sierdsema, A. Radović, A. Dilo, Spatial prediction of species' distributions from
699 occurrence -only records: Combining point pattern analysis, ENFA and regression-kriging.
700 *Ecol. Modell.* **220**, 3499–3511 (2009).

701 60. R. E. Schulze, "South African atlas of climatology and agrohydrology. Water Research
702 Commission, Pretoria, RSA, WRC Report 1489/1/06" (2007).

703 61. FAO/IIASA/ISRIC/ISSCAS/JRC, Harmonized World Soil Database (version 1.2) (2012).

704 62. P. Goldblatt, J. C. Manning, Cape Plants: A Conspectus of the Cape Flora of South Africa.
705 *Strelitzia* **9**, 1–743 (2000).

706 63. J. C. Manning, P. Goldblatt, *Plants of the Greater Cape Floristic Region 1: The Core Cape*
707 *flora* (South African National Biodiversity Institute, 2012).

708 64. R Core Team, R: A language and environment for statistical computing. R Foundation for
709 Statistical Computing (2018).

710 65. A. Baddeley, E. Rubak, R. Turner, *Spatial point patterns: Methodology and applications with*
711 *R* (Chapman and Hall/CRC Press, 2015).

66. E. J. Pebesma, R. S. Bivand, Classes and methods for spatial data in R. *R News* **5**, 9–13 (2005).

67. R. S. Bivand, E. Pebesma, V. Gomez-Rubio, *Applied spatial data analysis with R, Second edition*, Second (Springer, 2013).

68. R. Bivand, T. Keitt, B. Rowlingson, rgdal: Bindings for the "Geospatial" data abstraction library (2018).

69. B. Graler, E. Pebesma, G. Heuvelink, Spatio-temporal interpolation using gstat. *R J.* **8**, 204–218 (2016).

70. E. Paradis, Molecular dating of phylogenies by likelihood methods: A comparison of models and a new information criterion. *Mol. Phylogenet. Evol.* **67**, 436–444 (2013).

71. E. Paradis, K. Schliep, ape: analyses of phylogenetics and evolution in R language. *Bioinformatics* **20**, 289–290 (2004).

72. M. J. Sanderson, Estimating absolute rates of molecular evolution and divergence times: A penalized likelihood approach. *Mol. Biol. Evol.* **19**, 101–109 (2002).

73. M. Kearse, *et al.*, Geneious Basic: An integrated and extendable desktop software platform for the organization and analysis of sequence data. *Bioinformatics* **28**, 1647–1649 (2012).

74. R. C. Edgar, MUSCLE: multiple sequence alignment with high accuracy and high throughput. *Nucleic Acids Res.* **32**, 1792–1797 (2004).

75. G. A. Verboom, *et al.*, Origin and diversification of the Greater Cape flora: Ancient species repository, hot-bed of recent radiation, or both? *Mol. Phylogenet. Evol.* **51**, 44–53 (2009).

76. L. J. Revell, Phytools: An R package for phylogenetic comparative biology (and other things). *Methods Ecol. Evol.* **3**, 217–223 (2012).

77. A. J. Wilson, M.F.J., O'Connell, B., Brown, C., Guinan, J.C., Grehan, Multiscale terrain analysis of multibeam bathymetry data for habitat mapping on the continental slope. *Mar.*

Geod. **30**, 3–35 (2007).

78. S. Running, Q. Mu, M. Zao, A. Moreno, User's guide MODIS Global Terrestrial Evapotranspiration (ET) Product (NASA MOD16A2/A3) NASA Earth Observing System MODIS Land Algorithm. 1–35 (2017).

79. J. S. Singarayer, P. J. Valdes, High-latitude climate sensitivity to ice-sheet forcing over the last 120 kyr. *Quat. Sci. Rev.* **29**, 43–55 (2010).

80. C. Gordon, *et al.*, The simulation of SST, sea ice extents and ocean heat transports in a version of the Hadley Centre coupled model without flux adjustments. *Clim. Dyn.* **16**, 147–168 (2000).

81. M. Hutchinson, "A new objective method for spatial interpolation of meteorological variables from irregular networks applied to the estimation of monthly mean solar radiation, temperature, precipitation and windrun" (CSIRO Division of Water Resources, 1989).

82. M. G. New, M. Hulme, P. Jones, Representing twentieth century space-time climate variability. Part 1: Development of a 1961–90 mean monthly terrestrial climatology. *J. Clim.* **12**, 829–856 (1999).

83. J. Besag, J. York, A. Mollié, A Bayesian image restoration with two applications in spatial statistics. *Ann. Inst. Stat. Math.* **43**, 1–20 (1991).

84. H. Rue, S. Martino, N. Chopin, Approximate Bayesian inference for latent Gaussian models by using integrated nested Laplace approximations. *J. R. Stat. Soc. B* **71**, 319–392 (2009).

85. F. Lindgren, H. Rue, Bayesian spatial modelling with R-INLA. *J. Stat. Softw.* **63**, 1–25 (2015).

86. C. M. Beale, J. J. Lennon, J. M. Yearsley, M. J. Brewer, D. A. Elston, Regression analysis of spatial data. *Ecol. Lett.* **13**, 246–64 (2010).

Figure Legends

Fig.1. Hypothetical examples depicting the possible scenarios by which the ecological opportunity hypothesis, which focuses upon gradients in, for example, topographic diversity, seasonality and water–energy, and/or the age and area hypothesis, here considered in terms of late-Pleistocene climatic and biome stability, can explain plant diversity patterns in the CFR. Areas where both hypotheses would influence diversity achieve the highest values for all diversity metrics (Box A), except possibly for phylogenetic beta diversity (PBD), which value will vary depending on the proportion of range-restricted species and their distribution on the tree. In Box A, Scenario 1 has a high proportion of range-restricted, recently diverged species and thus a low PBD, while in Scenario 2 the range-restricted species are predominantly older, resulting in a higher PBD. The effect of the age and area hypothesis alone is shown in Box B, while the outcomes of the ecological opportunity hypothesis alone are depicted in Box C. In Boxes B and C, PBD will increase with higher proportions of range-restricted species, but will be less affected by the distribution of these species (contrary to the situation in Box A); range-restricted taxa are expected to be more prevalent in Box C. An area that is ecologically homogeneous and with unstable biome and climate (Box D) has the lowest diversity metrics. Black dots and circles depict the distribution on the phylogenetic tree of the species present in each scenario.

Fig. 2. Spatial patterns of the five predictor variables (A-E) plotted for the Cape Floristic Region (F).

Fig. 3. Spatial patterns of the four diversity variables (A-D) and of residuals from linear regressions of phylogenetic diversity on species richness (E) and of phylogenetic-beta diversity on taxonomic beta diversity (F), plotted for the Cape Floristic Region.

Fig. 4. The relationships between species richness predicted from models with (A) climate stability, (B) biome stability, (C) topographic heterogeneity, (D) energy, and (E) seasonality. Figure (F) shows simplified plots of the relationship of these covariates with the remaining diversity variables controlling for species richness (species turnover, phylogenetic and phylogenetic-beta diversity; See

SI Appendix, Fig. S4 for detailed plots). Within each plot, the results are shown with median estimate and 95% confidence intervals (shaded). Confidence intervals are computed from models that include all fixed and spatially explicit random effects: the presence of strong spatial effects generates wider scatter in the points than may be expected from plotted confidence intervals. A large asterisk indicates well-supported effects with confidence intervals that exclude zero; a small asterisk indicates that models excluding a specific covariate received more support from wAIC statistics than a full model including all covariates. For example, excluding climate stability or energy received more support from wAIC statistics than the full model suggesting the positive effects of biome stability and topographic heterogeneity and the negative effects of seasonality on species richness are the most robust. [phylo-diversity = phylogenetic diversity; phylo-beta diversity = phylogenetic beta diversity].

Tables and Legend

Table 1. Raw mean effects of the INLA analysis for raw diversity variables and controlling for the effects of species richness (SR). The set of historical and ecological covariates best explaining the spatial diversity patterns are shown by well-supported effects (in bold font) and wAIC values: shaded cells indicate a wAIC value increase of ≥3 when a covariate is removed from a model with a full set of covariates (See SI Appendix, Table S1 & S2 for full models results).

		Age and area		**Ecological opportunity**		
		Climate stability	Biome stability	Topographic heterogeneity	Productivity	Seasonality
Taxonomic diversity	Species richness	**0.110 (0.020, 0.200)**	**0.219 (0.109, 0.328)**	**0.078 (0.051, 0.105)**	**0.079 (0.024, 0.133)**	**-0.377 (-0.554, -0.120)**
	Beta diversity	0.001 (-0.128, 0.147)	0.112 (-0.056, 0.279)	**-0.111 (-0.141, -0.082)**	**-0.080 (-0.152, -0.008)**	**0.295 (0.046, 0.543)**
	Beta diversity SR	**0.134 (0.022, 0.247)**	**0.328 (0.191, 0.465)**	**-0.047 (-0.075, -0.018)**	-0.028 (-0.091, 0.035)	-0.163 (-0.375, 0.050)
Evolutionary diversity	Phylogenetic diversity	**0.107 (0.013, 0.202**)	**0.295 (0.179, 0.410)**	**0.083 (0.056, 0.111)**	**0.099 (0.043, 0.156)**	**-0.524 (-0.708, -0.339)**
	Phylogenetic diversitySR	0.022 (-0.032, 0.075)	**0.094 (0.029, 0.161)**	0.019 (-0.006, 0.044)	0.030 (-0.010, 0.070)	**-0.193 (-0.306, -0.079)**
	Phylogenetic beta diversity	0.0001 (-0.104, 0.103)	**-0.337 (-0.463, -0.210)**	**-0.086 (-0.114, -0.059)**	**-0.162 (-0.221, -0.102)**	**0.220 (0.021, 0.418)**
	Phylogenetic beta diversitySR	**0.120 (0.053, 0.187)**	**-0.173 (-0.255, -0.090)**	-0.018 (-0.044, 0.008)	**-0.090 (-0.136, -0.044)**	**-0.172 (-0.312, -0.032)**

[Medians with lower (0.025) and upper (0.975) quantiles are shown in brackets]

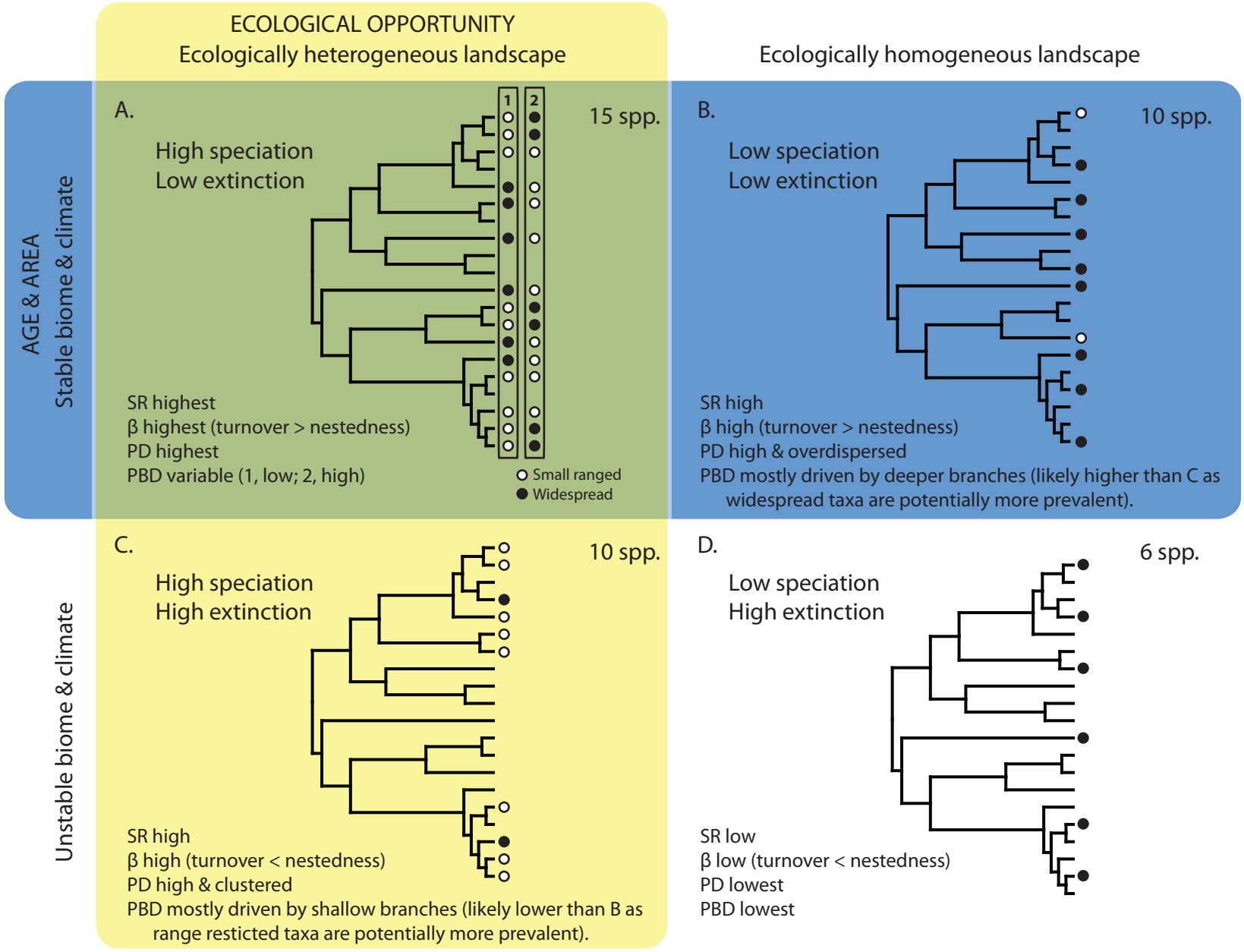

SR: species diversity β: beta diversity PD: phylogenetic diversity PBD: phylogenetic beta diversity

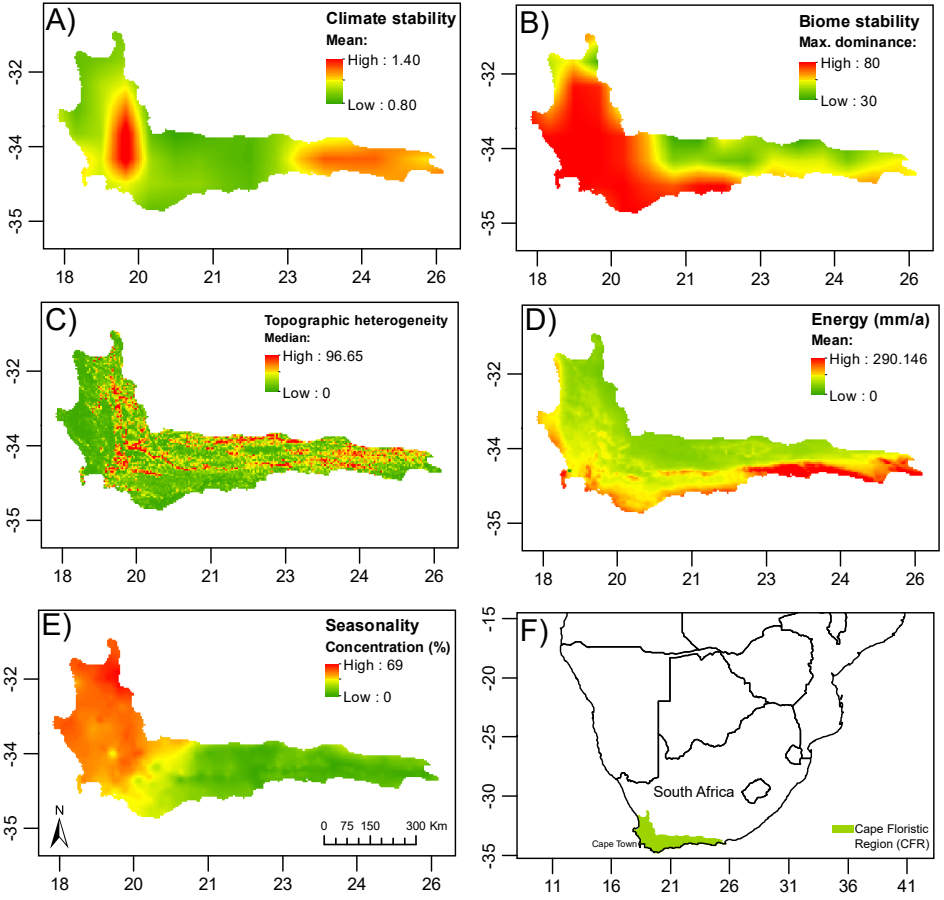
A)
Climate stability
Mean:
High : 1.40
Low : 0.80
B)
Biome stability
Max. dominance:
High : 80
Low : 30
C)
Topographic heterogeneity
Median:
High : 96.65
Low : 0
D)
Energy (mm/a)
Mean:
High : 290.146
Low : 0
E)
Seasonality
Concentration (%)
High : 69
Low : 0
N
0 75 150 300 Km
F)
South Africa
Cape Town
Cape Floristic Region (CFR)
-32
-34
-35
18
20
21
23
24
26
-15
-20
-25
-30
11
16
21
26
31
36
41

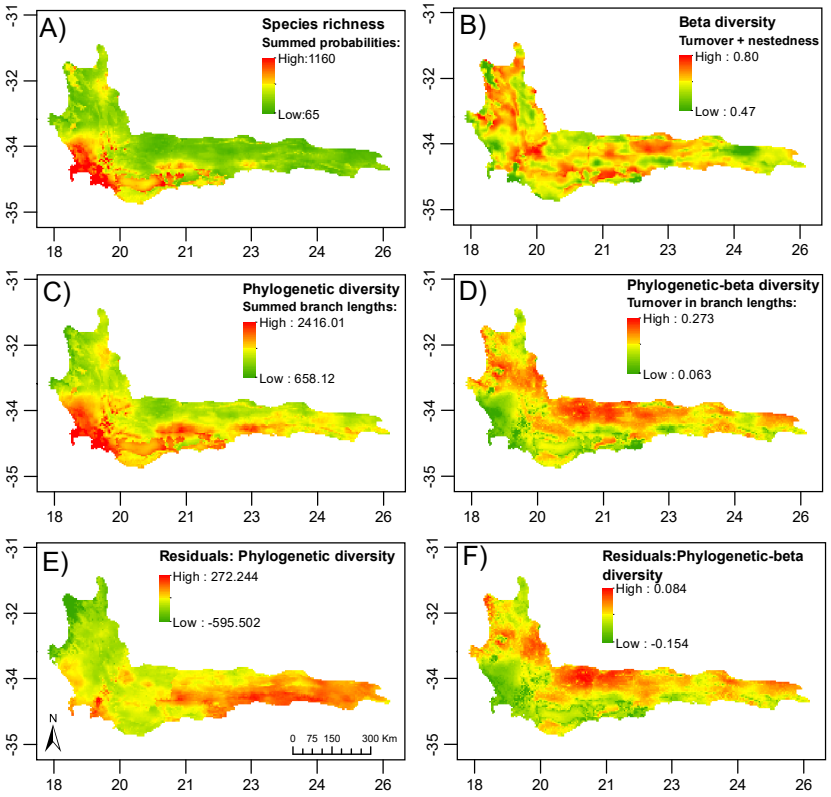
A)
Species richness
Summed probabilities:
High:1160
Low:65
B)
Beta diversity
Turnover + nestedness
High : 0.80
Low : 0.47
C)
Phylogenetic diversity
Summed branch lengths:
High : 2416.01
Low : 658.12
D)
Phylogenetic-beta diversity
Turnover in branch lengths:
High : 0.273
Low : 0.063
E)
Residuals: Phylogenetic diversity
High : 272.244
Low : -595.502
N
0 75 150 300 Km
F)
Residuals:Phylogenetic-beta diversity
High : 0.084
Low : -0.154
-31
-32
-34
-35
18
20
21
23
24
26

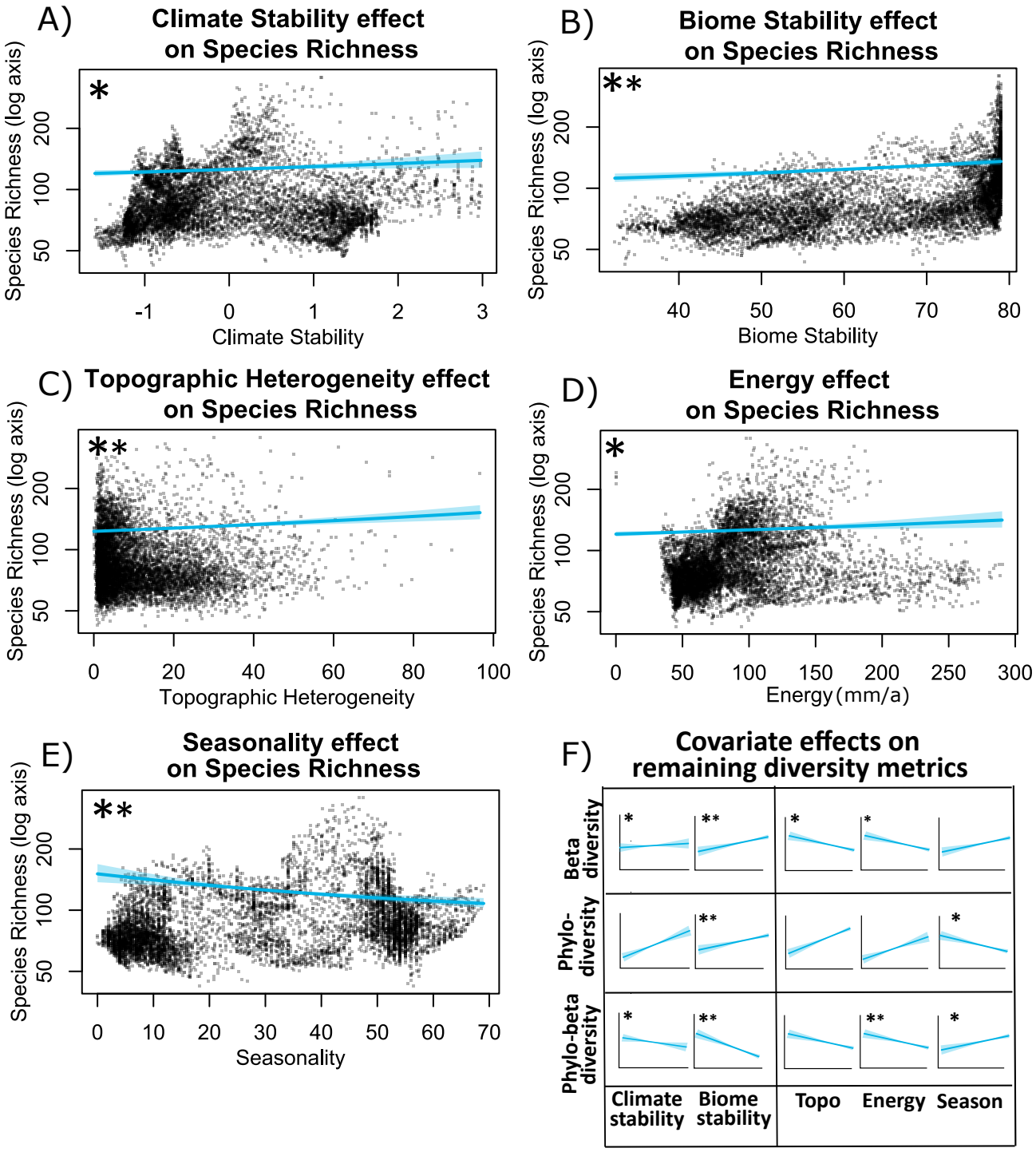
A)
Climate Stability effect on Species Richness
Species Richness (log axis)
Climate Stability
B)
Biome Stability effect on Species Richness
Biome Stability
C)
Topographic Heterogeneity effect on Species Richness
Topographic Heterogeneity
D)
Energy effect on Species Richness
Energy (mm/a)
E)
Seasonality effect on Species Richness
Seasonality
F)
Covariate effects on remaining diversity metrics
Beta diversity
Phylo-diversity
Phylo-beta diversity
Climate stability
Biome stability
Topo
Energy
Season

Supporting Information

Fig S1. (A) Total CFR plant species, (B) Cape clade species and (C) the Cape clade species included in our phylogeny show (D) strongly correlated spatial patterns of richness with each other (r~0.9).

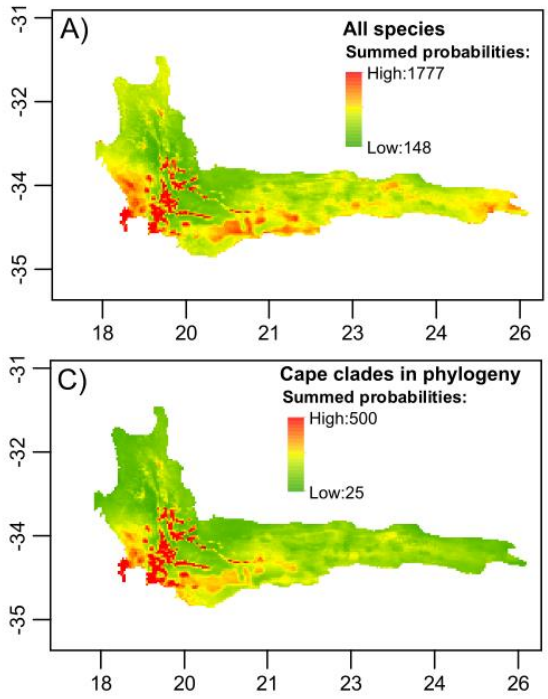

D)

Correlation matrix	All species	Cape clades	Cape clades in phylogeny
All species	1.000	0.895	0.876
Cape clades	0.895	1.000	0.982
Cape clades in phylogeny	0.876	0.982	1.000

Fig. S2. Rainfall seasonality regions over South Africa following Schulze & Maharaj (2007).

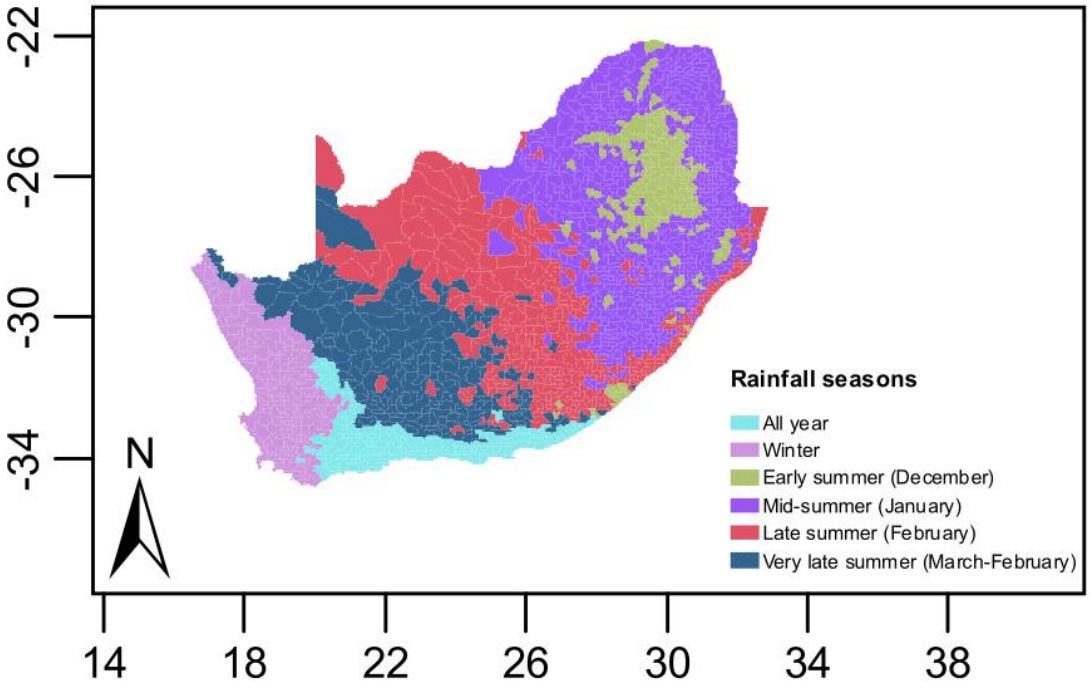

[Schulze, R.E. and Maharaj, M. 2007. Rainfall Seasonality. In: Schulze, R.E. (Ed). 2007. South African Atlas of Climatology and Agrohydrology. Water Research Commission, Pretoria, RSA, WRC Report 1489/1/06, Section 6.5.]

Fig S3. Spatial patterns of (A) species turnover and (B) nestedness plotted for the Cape Floristic Region. Taxonomic beta diversity was dominated by species turnover for the CFR, with nestedness making up only a small proportion of total taxonomic beta diversity.

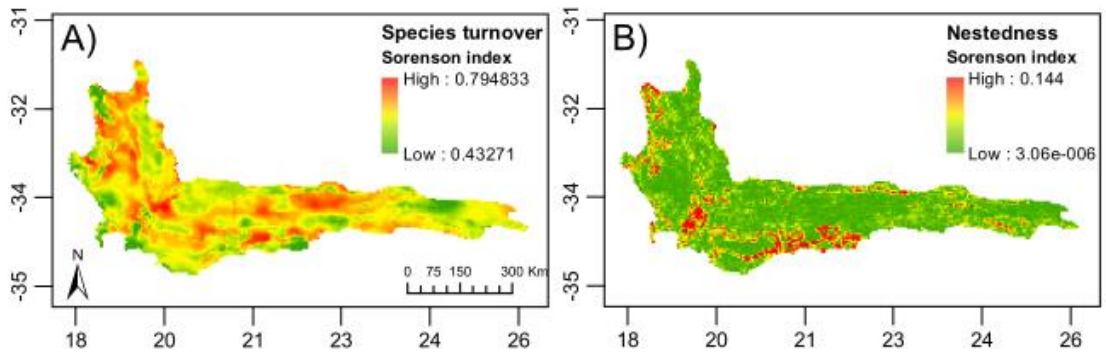

Table S1. wAIC values for the full model with all five covariates, and for models where a single covariate is removed. Grey shading indicates the importance of a covariate with an increase of ≥3 in the wAIC value when removed from the model with the lowest wAIC (shown in bold font)]. wAIC is a measure of model support equivalent to the well-known AIC score but appropriate to Bayesian models that can be used to compare relative support for different models of the same data. Deviance information criterion (dic) values, a Bayesian alternative to Akaike's information criterion (AIC), are also given. [Full model = climatic stability + biome stability + topographic heterogeneity + productivity + seasonality; SR = model controlling for the effects of species richness.]

	Model	wAIC	dic	Difference between model with lowest wAIC
Species richness	Full model	16020.02074	16396.06631	1.048
	Full model – climatic stability	16020.79628	16399.70405	1.823
	Full model – biome stability	16023.5865	16407.49952	4.614
	Full model – productivity	**16018.9728**	16400.69428	--
	Full model – seasonality	16029.73992	16410.44291	10.767
	Full model – topographic heterogeneity	16050.12553	16425.61027	31.153
Taxonomic beta diversity	Full model	17041.62868	17798.26508	0.980
	Full model – climatic stability	17041.21901	17797.33856	0.570
	Full model – biome stability	17041.24787	17798.5425	0.599
	Full model – productivity	**17040.64871**	17800.2544	--
	Full model – seasonality	17049.17655	17803.02755	8.528
	Full model – topographic heterogeneity	17064.87193	17841.74798	24.223
	Full modelSR	16013.46376	16612.4569	3.035
	Full model – climatic stabilitySR	**16010.42889**	16615.04852	--
	Full model – biome stabilitySR	16017.56591	16628.92278	7.137
	Full model – productivitySR	16013.43766	16611.79949	3.009
	Full model – seasonalitySR	16010.51185	16612.3853	0.083
	Full model – topographic heterogeneitySR	16013.54935	16618.77517	3.120
Phylogenetic diversity	Full model	**15926.48838**	16353.83571	--
	Full model – climatic stability	15926.86926	16356.74216	0.381
	Full model – biome stability	15933.324	16373.34072	6.836
	Full model – productivity	15927.00528	16361.82408	0.517
	Full model – seasonality	15943.04467	16379.95724	16.556
	Full model – topographic heterogeneity	15956.00152	16386.46558	29.513
	Full modelSR	14651.41871	14770.87755	1.283
	Full model – climatic stabilitySR	**14650.1358**	14769.8164	--
	Full model – biome stabilitySR	14654.26908	14776.59751	4.133
	Full model – productivitySR	14652.53905	14771.2953	2.403
	Full model – seasonalitySR	14652.8451	14778.6903	2.709
	Full model – topographic heterogeneitySR	14651.16078	14770.83809	1.025
Phylogenetic-beta diversity	Full model	16448.12959	16926.18894	0.358
	Full model – climatic stability	**16447.7712**	16925.16497	--
	Full model – biome stability	16450.84972	16945.98474	3.079
	Full model – productivity	16459.3285	16948.50771	11.557
	Full model – seasonality	16452.88221	16929.73907	5.111
	Full model – topographic heterogeneity	16478.44714	16959.88247	30.676
	Full modelSR	15567.37618	15766.48978	0.414
	Full model – climatic stabilitySR	**15566.96256**	15774.92335	--
	Full model – biome stabilitySR	15571.87702	15779.6292	4.914
	Full model – productivitySR	15579.72643	15779.45668	12.764
	Full model – seasonalitySR	15567.0543	15769.84668	0.092
	Full model – topographic heterogeneitySR	15569.18265	15766.63675	2.220

Fig. S4. The relationships between plant diversity variables predicted from models with climate stability, biome stability, topographic heterogeneity, productivity, and seasonality. Within each plot, the results are shown with median estimate and 95% confidence intervals (shaded). Confidence intervals are computed from models that include all fixed and spatially explicit random effects: the presence of strong spatial effects generates wider scatter in the points than may be expected from plotted confidence intervals. [PD = phylogenetic diversity; PBD = phylogenetic beta diversity; Sorenson Beta-diversity = beta diversity]. These plots should be read in conjunction with Table S1.

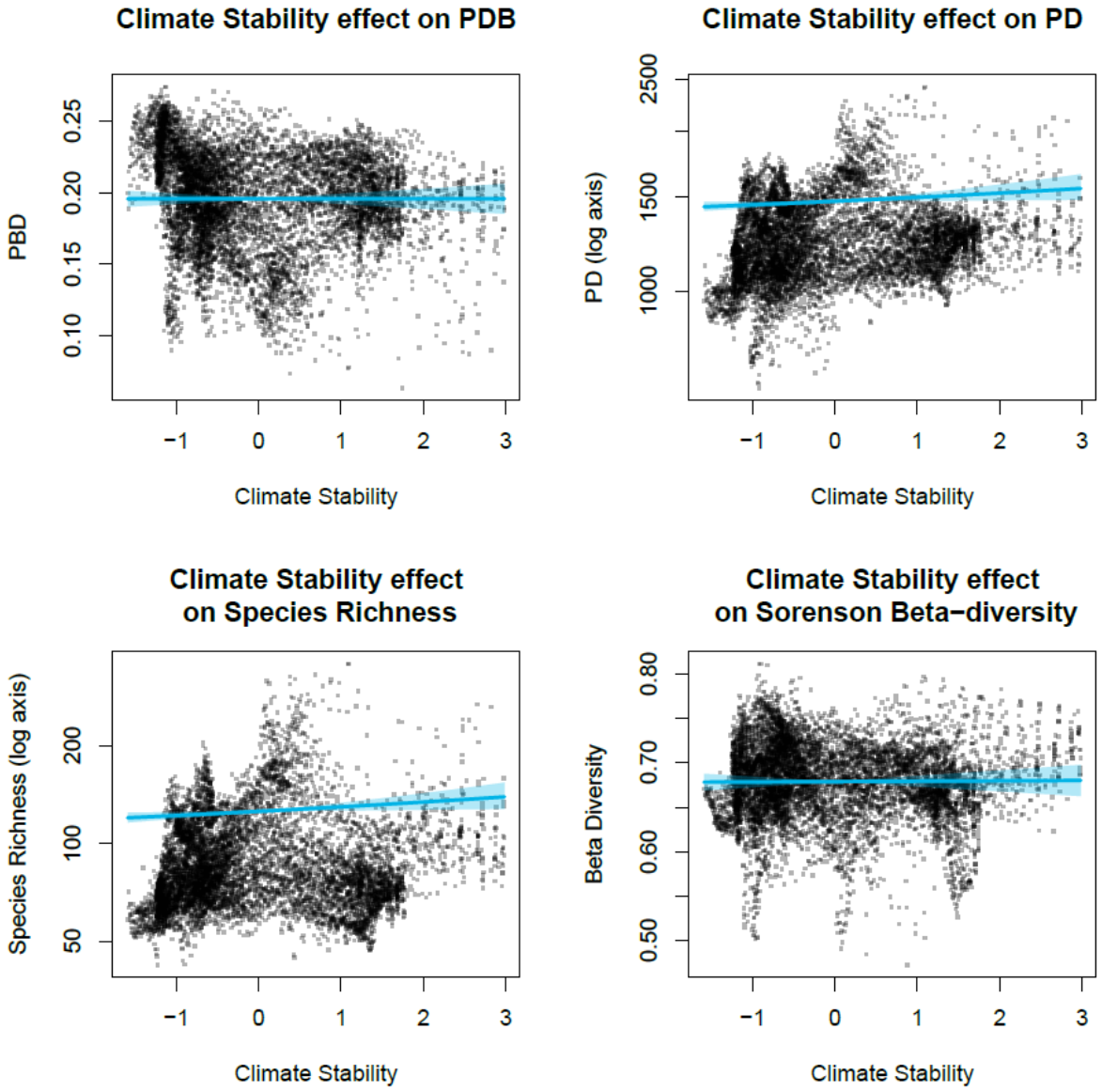

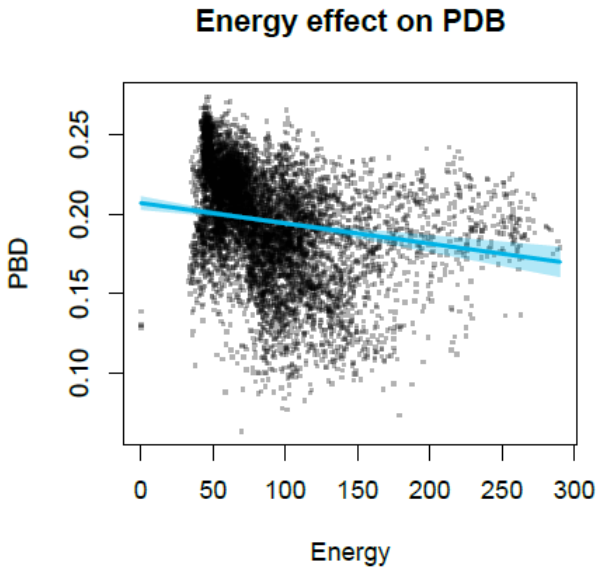
Energy effect on PDB
PBD
0.10
0.15
0.20
0.25
0
50
100
150
200
250
300
Energy

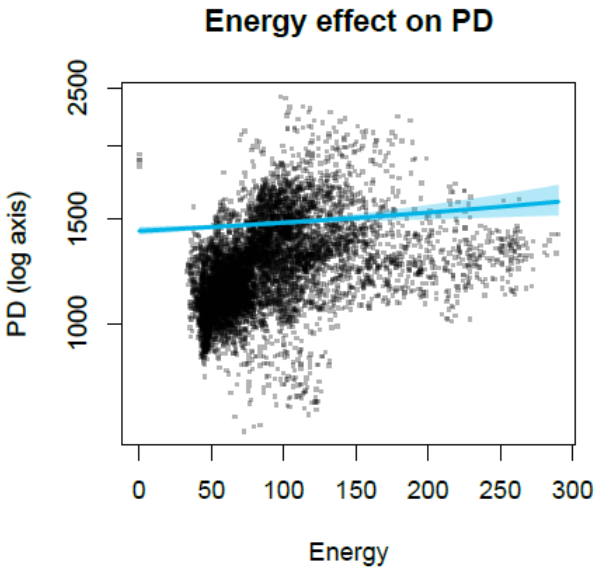
Energy effect on PD
PD (log axis)
1000
1500
2500
0
50
100
150
200
250
300
Energy

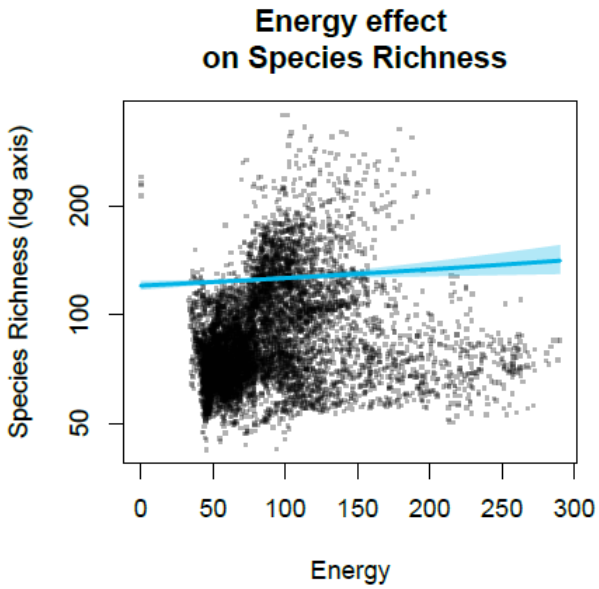
Energy effect
on Species Richness
Species Richness (log axis)
50
100
200
0
50
100
150
200
250
300
Energy

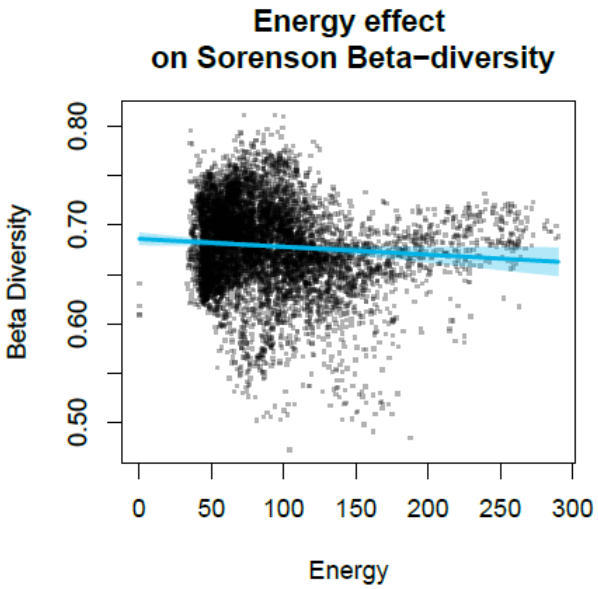
Energy effect
on Sorenson Beta−diversity
Beta Diversity
0.50
0.60
0.70
0.80
0
50
100
150
200
250
300
Energy

34

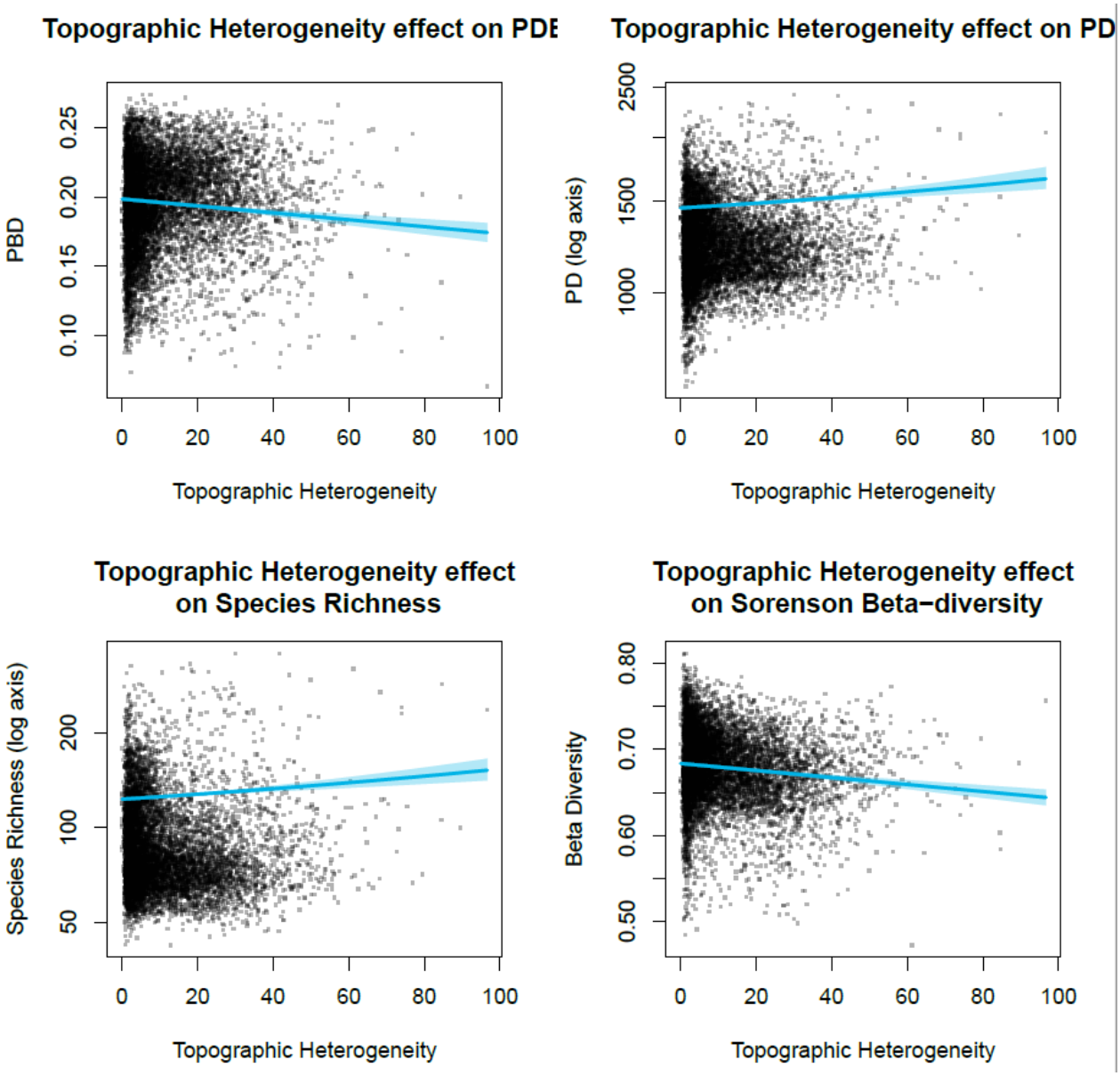
Topographic Heterogeneity effect on PDE
PBD
0.10
0.15
0.20
0.25
0
20
40
60
80
100
Topographic Heterogeneity
Topographic Heterogeneity effect on PD
PD (log axis)
1000
1500
2500
0
20
40
60
80
100
Topographic Heterogeneity
Topographic Heterogeneity effect on Species Richness
Species Richness (log axis)
50
100
200
0
20
40
60
80
100
Topographic Heterogeneity
Topographic Heterogeneity effect on Sorenson Beta−diversity
Beta Diversity
0.50
0.60
0.70
0.80
0
20
40
60
80
100
Topographic Heterogeneity

35

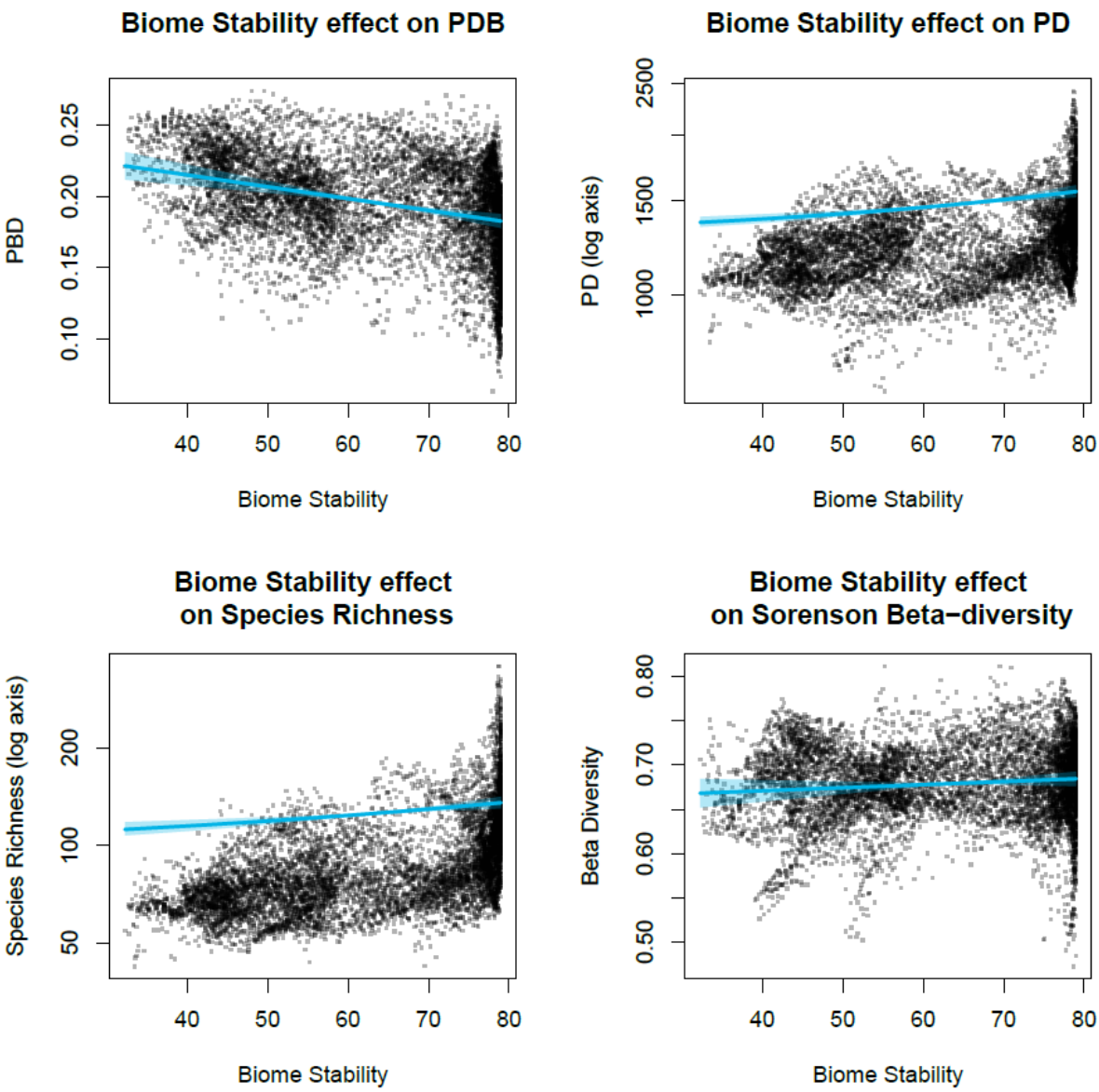
Biome Stability effect on PDB
PBD
0.10
0.15
0.20
0.25
40
50
60
70
80
Biome Stability
Biome Stability effect on PD
PD (log axis)
1000
1500
2500
40
50
60
70
80
Biome Stability
Biome Stability effect
on Species Richness
Species Richness (log axis)
50
100
200
40
50
60
70
80
Biome Stability
Biome Stability effect
on Sorenson Beta-diversity
Beta Diversity
0.50
0.60
0.70
0.80
40
50
60
70
80
Biome Stability

36

37

Table S2. INLA model fixed effects summaries for each diversity model run, and for models controlling for species richness (SR). Pseudo-R^2 values are given for each of the full models incorporating all five covariates. Joint estimation of the spatial error term and fixed effects enables accurate computation of fixed effects but the relatively strong spatial effects modelled mean comparison of the raw data with the confidence intervals of the parameters may be misleading: to the naïve eye, confidence intervals may be more precisely estimated than raw data seems to imply possible.

Species richness: Full model (pseudo-R^2 = 0.922)	mean	sd	0.025 quantile	0.5 quantile	0.975 quantile
(Intercept)	2.95E-10	0.01135	-0.02228	-3.19E-07	0.022265
climatic stability	0.110318	0.045802	0.020324	0.110333	0.200147
biome stability	0.218661	0.055949	0.108722	0.218681	0.328382
topographic heterogeneity	0.0777	0.013758	0.05069	0.0777	0.10469
productivity	0.078684	0.027898	0.023823	0.078711	0.133344
seasonality	-0.3768	0.090239	-0.55405	-0.37678	-0.1998
Species richness: Full model – climatic stability	mean	sd	0.025 quantile	0.5 quantile	0.975 quantile
(Intercept)	2.95E-10	0.01135	-0.02228	-3.19E-07	0.022265
biome stability	0.251593	0.054439	0.144605	0.251618	0.358339
topographic heterogeneity	0.081068	0.013695	0.05418	0.081068	0.107933
productivity	0.074932	0.027927	0.020016	0.07496	0.129649
seasonality	-0.35949	0.090221	-0.53674	-0.35947	-0.18256
Species richness: Full model – biome stability	mean	sd	0.025 quantile	0.5 quantile	0.975 quantile
(Intercept)	3.07E-10	0.01135	-0.02228	-3.19E-07	0.022265
climatic stability	0.153947	0.044844	0.065824	0.153966	0.241884
topographic heterogeneity	0.074893	0.013761	0.047877	0.074892	0.10189
productivity	0.116109	0.026349	0.064245	0.116151	0.167691
seasonality	-0.36328	0.090891	-0.54185	-0.36325	-0.18504
Species richness: Full model – productivity	mean	sd	0.025 quantile	0.5 quantile	0.975 quantile
(Intercept)	3.36E-10	0.01135	-0.02228	-3.19E-07	0.022265
climatic stability	0.103429	0.04607	0.012908	0.103445	0.193782
biome stability	0.273936	0.052767	0.170145	0.273991	0.377326
topographic heterogeneity	0.079022	0.013766	0.051995	0.079021	0.106027
seasonality	-0.4186	0.089529	-0.59438	-0.41862	-0.24293
Species richness: Full model – seasonality	mean	sd	0.025 quantile	0.5 quantile	0.975 quantile
(Intercept)	1.83E-11	0.01135	-0.02228	-3.20E-07	0.022265
climatic stability	0.094774	0.045959	0.004485	0.094784	0.184922
biome stability	0.209097	0.056273	0.098546	0.209109	0.319475
topographic heterogeneity	0.079444	0.013767	0.052417	0.079443	0.106451
productivity	0.097205	0.02766	0.042796	0.097237	0.151385
Species richness: Full model – topographic heterogeneity	mean	sd	0.025 quantile	0.5 quantile	0.975 quantile
(Intercept)	3.14E-10	0.01135	-0.02228	-3.19E-07	0.022265
climatic stability	0.136571	0.04566	0.046856	0.136585	0.226123

biome stability	0.201623	0.055986	0.091603	0.201647	0.311411
productivity	0.083788	0.027905	0.028922	0.083813	0.138471
seasonality	-0.39212	0.090358	-0.56965	-0.39209	-0.21493
Taxonomic beta diversity: Full model (pseudo-R^2 = 0.924)	mean	sd	0.025 quantile	0.5 quantile	0.975 quantile
(Intercept)	-2.51E-10	0.01135	-0.02228	-3.20E-07	0.022265
climatic stability	0.009601	0.070171	-0.12828	0.00963	0.147194
biome stability	0.111702	0.085325	-0.05588	0.111712	0.279075
topographic heterogeneity	-0.11146	0.01497	-0.14084	-0.11147	-0.08208
productivity	-0.08014	0.036724	-0.15221	-0.08015	-0.00806
seasonality	0.294752	0.126702	0.046265	0.294648	0.543587
Taxonomic beta diversity: Full model – climatic stability	mean	sd	0.025 quantile	0.5 quantile	0.975 quantile
(Intercept)	-2.38E-10	0.01135	-0.02228	-3.20E-07	0.022265
biome stability	0.114552	0.082759	-0.04802	0.114572	0.276867
topographic heterogeneity	-0.11133	0.014928	-0.14063	-0.11134	-0.08203
productivity	-0.08047	0.036643	-0.15238	-0.08049	-0.00855
seasonality	0.295689	0.126434	0.047719	0.295588	0.543991
Taxonomic beta diversity: Full model – biome stability	mean	sd	0.025 quantile	0.5 quantile	0.975 quantile
(Intercept)	-2.47E-10	0.01135	-0.02228	-3.20E-07	0.022265
climatic stability	0.031826	0.068114	-0.10203	0.031858	0.165377
topographic heterogeneity	-0.11225	0.01496	-0.14161	-0.11226	-0.08289
productivity	-0.06578	0.035059	-0.13459	-0.06579	0.003024
seasonality	0.298034	0.12672	0.049504	0.297932	0.546897
Taxonomic beta diversity: Full model – productivity	mean	sd	0.025 quantile	0.5 quantile	0.975 quantile
(Intercept)	-2.66E-10	0.01135	-0.02228	-3.20E-07	0.022265
climatic stability	0.019151	0.070181	-0.11875	0.01918	0.156763
biome stability	0.056181	0.081623	-0.10409	0.056176	0.216331
topographic heterogeneity	-0.1128	0.014963	-0.14216	-0.11281	-0.08343
seasonality	0.331643	0.125795	0.084906	0.331549	0.578671
Taxonomic beta diversity: Full model – seasonality	mean	sd	0.025 quantile	0.5 quantile	0.975 quantile
(Intercept)	-1.90E-12	0.01135	-0.02228	-3.20E-07	0.022265
climatic stability	0.019456	0.069971	-0.11803	0.019483	0.156663
biome stability	0.115483	0.085224	-0.05191	0.115494	0.282656
topographic heterogeneity	-0.11299	0.014951	-0.14232	-0.11299	-0.08364
productivity	-0.0914	0.036378	-0.1628	-0.09142	-0.02
Taxonomic beta diversity: Full model – topographic heterogeneity	mean	sd	0.025 quantile	0.5 quantile	0.975 quantile
(Intercept)	-2.71E-10	0.01135	-0.02228	-3.20E-07	0.022265
climatic stability	-0.02883	0.071091	-0.16849	-0.02881	0.110592
biome stability	0.137732	0.086582	-0.03233	0.137745	0.307564
productivity	-0.09169	0.037071	-0.16445	-0.09171	-0.01893
seasonality	0.3402	0.128199	0.088783	0.340093	0.591978
Taxonomic beta diversity: Full model.SR (pseudo-R^2 = 0.948)	mean	sd	0.025 quantile	0.5 quantile	0.975 quantile
(Intercept)	13.87861	0.372267	13.14779	13.87857	14.60896

climatic stability	0.134676	0.057272	0.022041	0.134732	0.246892
biome stability	0.328313	0.069891	0.190997	0.328337	0.465373
topographic heterogeneity	-0.0466	0.014486	-0.07503	-0.0466	-0.01817
productivity	-0.02796	0.032115	-0.09102	-0.02796	0.035043
seasonality	-0.16241	0.108194	-0.37453	-0.16252	0.05014
log(SR)	-3.1164	0.083553	-3.28046	-3.11639	-2.9525
Taxonomic beta diversity: Full model – climatic stability.SR	mean	sd	0.025 quantile	0.5 quantile	0.975 quantile
(Intercept)	13.8369	0.372437	13.10579	13.83685	14.56763
biome stability	0.367212	0.068176	0.233216	0.367251	0.500865
topographic heterogeneity	-0.04379	0.014446	-0.07215	-0.0438	-0.01545
productivity	-0.03268	0.032143	-0.0958	-0.03268	0.030376
seasonality	-0.14264	0.108233	-0.35488	-0.14274	0.069951
log(SR)	-3.10703	0.083591	-3.27118	-3.10703	-2.94307
Taxonomic beta diversity: Full model – biome stability.SR	mean	sd	0.025 quantile	0.5 quantile	0.975 quantile
(Intercept)	13.74174	0.372543	13.01045	13.74167	14.4727
climatic stability	0.197368	0.056205	0.086823	0.197427	0.307485
topographic heterogeneity	-0.04995	0.014498	-0.0784	-0.04995	-0.02149
productivity	0.019501	0.030686	-0.04079	0.019514	0.079667
seasonality	-0.14168	0.108974	-0.35537	-0.14177	0.072368
log(SR)	-3.08566	0.083615	-3.24986	-3.08565	-2.92166
Taxonomic beta diversity: Full model – productivity.SR	mean	sd	0.025 quantile	0.5 quantile	0.975 quantile
(Intercept)	13.89564	0.371728	13.16587	13.89561	14.62493
climatic stability	0.137801	0.057149	0.025411	0.137857	0.249781
biome stability	0.308992	0.066261	0.178794	0.309019	0.438925
topographic heterogeneity	-0.04702	0.014477	-0.07543	-0.04703	-0.01861
seasonality	-0.14939	0.107133	-0.35942	-0.1495	0.061085
log(SR)	-3.12022	0.083431	-3.28405	-3.12022	-2.95656
Taxonomic beta diversity: Full model – seasonality.SR	mean	sd	0.025 quantile	0.5 quantile	0.975 quantile
(Intercept)	13.82605	0.370941	13.0979	13.826	14.55386
climatic stability	0.128131	0.057242	0.015576	0.12818	0.240307
biome stability	0.324548	0.07001	0.187013	0.324565	0.461856
topographic heterogeneity	-0.04599	0.014487	-0.07442	-0.04599	-0.01756
productivity	-0.02129	0.031857	-0.08386	-0.02129	0.041188
log(SR)	-3.1046	0.083255	-3.26809	-3.10459	-2.9413
Taxonomic beta diversity: Full model – topographic heterogeneity.SR	mean	sd	0.025 quantile	0.5 quantile	0.975 quantile
(Intercept)	14.0495	0.369197	13.32463	14.04949	14.77377
climatic stability	0.119832	0.057401	0.006964	0.119881	0.232321
biome stability	0.340947	0.070157	0.203095	0.340974	0.478517
productivity	-0.03143	0.032212	-0.09468	-0.03143	0.031761
seasonality	-0.15261	0.108637	-0.3656	-0.15273	0.060807
log(SR)	-3.15477	0.082863	-3.31746	-3.15477	-2.99221
Phylogenetic diversity: Full model (pseudo-R^2 = 0.934)	mean	sd	0.025 quantile	0.5 quantile	0.975 quantile

(Intercept)	4.08E-10	0.01135	-0.02228	-3.19E-07	0.022265
climatic stability	0.107332	0.048229	0.012568	0.107348	0.201916
biome stability	0.294842	0.058892	0.179128	0.294862	0.410335
topographic heterogeneity	0.083446	0.013878	0.056196	0.083447	0.110668
productivity	0.099357	0.028815	0.042705	0.099381	0.155823
seasonality	-0.52358	0.094012	-0.70821	-0.52358	-0.33916
Phylogenetic diversity: Full model – climatic stability	mean	sd	0.025 quantile	0.5 quantile	0.975 quantile
(Intercept)	4.59E-10	0.01135	-0.02228	-3.19E-07	0.022265
biome stability	0.326839	0.057265	0.214305	0.326865	0.439126
topographic heterogeneity	0.086408	0.013822	0.059266	0.08641	0.11352
productivity	0.095674	0.028826	0.039	0.095698	0.152163
seasonality	-0.5075	0.093955	-0.69204	-0.50749	-0.32321
log(SR)	4.59E-10	0.01135	-0.02228	-3.19E-07	0.022265
Phylogenetic diversity: Full model – biome stability	mean	sd	0.025 quantile	0.5 quantile	0.975 quantile
(Intercept)	4.03E-10	0.01135	-0.02228	-3.19E-07	0.022265
climatic stability	0.165955	0.047434	0.072743	0.165976	0.258969
topographic heterogeneity	0.079737	0.013891	0.052462	0.079737	0.106986
productivity	0.147587	0.02738	0.093705	0.147627	0.201198
seasonality	-0.50709	0.095031	-0.69376	-0.50707	-0.32071
Phylogenetic diversity: Full model – productivity	mean	sd	0.025 quantile	0.5 quantile	0.975 quantile
(Intercept)	4.47E-10	0.01135	-0.02228	-3.19E-07	0.022265
climatic stability	0.098022	0.048566	0.002595	0.09804	0.193264
biome stability	0.364493	0.05577	0.254819	0.364544	0.473783
topographic heterogeneity	0.085043	0.013889	0.057771	0.085044	0.112286
seasonality	-0.57499	0.093448	-0.75844	-0.57501	-0.39161
Phylogenetic diversity: Full model – seasonality	mean	sd	0.025 quantile	0.5 quantile	0.975 quantile
(Intercept)	2.19E-11	0.01135	-0.02228	-3.20E-07	0.022265
climatic stability	0.086277	0.04866	-0.00931	0.086287	0.181722
biome stability	0.282514	0.059548	0.165541	0.282524	0.39932
topographic heterogeneity	0.085753	0.013898	0.058463	0.085754	0.113015
productivity	0.123782	0.028694	0.067352	0.123812	0.179996
Phylogenetic diversity: Full model – topographic heterogeneity	mean	sd	0.025 quantile	0.5 quantile	0.975 quantile
(Intercept)	4.55E-10	0.01135	-0.02228	-3.19E-07	0.022265
climatic stability	0.135363	0.048294	0.040466	0.135382	0.230068
biome stability	0.276184	0.059166	0.159929	0.276205	0.392213
productivity	0.105097	0.028895	0.048296	0.105118	0.161729
seasonality	-0.54171	0.09442	-0.72717	-0.54169	-0.35652
Phylogenetic diversity: Full model.SR (pseudo-R^2 = 0.984)	mean	sd	0.025 quantile	0.5 quantile	0.975 quantile
(Intercept)	-13.2888	0.274862	-13.8279	-13.2891	-12.749
biome stability	0.101016	0.032649	0.036801	0.101044	0.165018
topographic heterogeneity	0.020471	0.012753	-0.00458	0.020475	0.045477
productivity	0.029161	0.020377	-0.01083	0.029154	0.069156
seasonality	-0.18626	0.057174	-0.29833	-0.18635	-0.07384

log(SR)	2.983968	0.061667	2.862731	2.984016	3.104822
Phylogenetic diversity: Full model – climatic stability.SR	mean	sd	0.025 quantile	0.5 quantile	0.975 quantile
(Intercept)	-13.2888	0.274862	-13.8279	-13.2891	-12.749
biome stability	0.101016	0.032649	0.036801	0.101044	0.165018
topographic heterogeneity	0.020471	0.012753	-0.00458	0.020475	0.045477
productivity	0.029161	0.020377	-0.01083	0.029154	0.069156
seasonality	-0.18626	0.057174	-0.29833	-0.18635	-0.07384
log(SR)	2.983968	0.061667	2.862731	2.984016	3.104822
Phylogenetic diversity: Full model – biome stability.SR	mean	sd	0.025 quantile	0.5 quantile	0.975 quantile
(Intercept)	-13.3787	0.274359	-13.9166	-13.3789	-12.8397
climatic stability	0.039474	0.026878	-0.01353	0.039546	0.092036
topographic heterogeneity	0.015418	0.012823	-0.00977	0.01542	0.040567
productivity	0.052852	0.018713	0.016089	0.052856	0.089553
seasonality	-0.17279	0.057747	-0.28604	-0.17286	-0.05929
log(SR)	3.004133	0.061554	2.883082	3.004194	3.124736
Phylogenetic diversity: Full model – productivity.SR	mean	sd	0.025 quantile	0.5 quantile	0.975 quantile
(Intercept)	-13.3189	0.273588	-13.8555	-13.3191	-12.7816
climatic stability	0.020813	0.027417	-0.03327	0.020892	0.074416
biome stability	0.11447	0.030644	0.054288	0.114463	0.174625
topographic heterogeneity	0.018716	0.012869	-0.00656	0.018719	0.043956
seasonality	-0.21107	0.056293	-0.32131	-0.21119	-0.10029
log(SR)	2.990712	0.06138	2.870052	2.990754	3.111019
Phylogenetic diversity: Full model – seasonality.SR	mean	sd	0.025 quantile	0.5 quantile	0.975 quantile
(Intercept)	-13.3691	0.2766	-13.9115	-13.3694	-12.8259
climatic stability	0.008103	0.027592	-0.04623	0.008146	0.062138
biome stability	0.081668	0.033918	0.01512	0.081641	0.148299
topographic heterogeneity	0.018673	0.012903	-0.00667	0.018676	0.043978
productivity	0.044155	0.020097	0.004664	0.044164	0.083563
log(SR)	3.001993	0.062057	2.879983	3.002044	3.123605
Phylogenetic diversity: Full model – topographic heterogeneity.SR	mean	sd	0.025 quantile	0.5 quantile	0.975 quantile
(Intercept)	-13.3069	0.274852	-13.8462	-13.3071	-12.7673
climatic stability	0.027528	0.02722	-0.02618	0.027611	0.080734
biome stability	0.090046	0.033479	0.024279	0.090047	0.155746
productivity	0.02912	0.020396	-0.01091	0.029111	0.069158
seasonality	-0.19269	0.057852	-0.306	-0.1928	-0.07887
log(SR)	2.988025	0.061664	2.866841	2.988057	3.108914
Phylogenetic beta diversity: Full model (pseudo-R^2 = 0.910)	mean	sd	0.025 quantile	0.5 quantile	0.975 quantile
(Intercept)	-1.88E-10	0.01135	-0.02228	-3.20E-07	0.022265
climatic stability	-0.00019	0.052834	-0.10401	-0.00018	0.103416
biome stability	-0.337	0.064485	-0.4635	-0.33704	-0.21036
topographic heterogeneity	-0.08643	0.014099	-0.11411	-0.08643	-0.05877
productivity	-0.16194	0.030499	-0.22179	-0.16195	-0.10208
seasonality	0.219788	0.101125	0.021441	0.219708	0.418387

Phylogenetic beta diversity: Full model – climatic stability	mean	sd	0.025 quantile	0.5 quantile	0.975 quantile
(Intercept)	-2.06E-10	0.01135	-0.02228	-3.20E-07	0.022265
biome stability	-0.3371	0.062484	-0.45969	-0.33714	-0.2144
topographic heterogeneity	-0.08644	0.014039	-0.114	-0.08644	-0.05889
productivity	-0.16195	0.030438	-0.22169	-0.16197	-0.10221
seasonality	0.219666	0.100813	0.021927	0.219589	0.417649

Phylogenetic beta diversity: Full model – biome stability	mean	sd	0.025 quantile	0.5 quantile	0.975 quantile
(Intercept)	-1.85E-10	0.01135	-0.02228	-3.20E-07	0.022265
climatic stability	-0.06815	0.052108	-0.17051	-0.06814	0.034063
topographic heterogeneity	-0.08271	0.014124	-0.11044	-0.08271	-0.055
productivity	-0.21373	0.029146	-0.27087	-0.21376	-0.15647
seasonality	0.207022	0.102482	0.006043	0.206933	0.40831

Phylogenetic beta diversity: Full model – productivity	mean	sd	0.025 quantile	0.5 quantile	0.975 quantile
(Intercept)	-2.57E-10	0.01135	-0.02228	-3.20E-07	0.022265
climatic stability	0.015609	0.053396	-0.08929	0.015622	0.12034
biome stability	-0.44987	0.061598	-0.57066	-0.44994	-0.32885
topographic heterogeneity	-0.0892	0.014119	-0.11692	-0.0892	-0.0615
seasonality	0.302598	0.100917	0.104599	0.30254	0.500734

Phylogenetic beta diversity: Full model – seasonality	mean	sd	0.025 quantile	0.5 quantile	0.975 quantile
(Intercept)	-2.29E-11	0.01135	-0.02228	-3.20E-07	0.022265
climatic stability	0.008125	0.052666	-0.09536	0.008144	0.11141
biome stability	-0.33266	0.064416	-0.45903	-0.33271	-0.20616
topographic heterogeneity	-0.08749	0.014088	-0.11515	-0.08749	-0.05985
productivity	-0.17199	0.030137	-0.23113	-0.172	-0.11283

Phylogenetic beta diversity: Full model – topographic heterogeneity	mean	sd	0.025 quantile	0.5 quantile	0.975 quantile
(Intercept)	-2.33E-10	0.01135	-0.02228	-3.20E-07	0.022265
climatic stability	-0.02968	0.052941	-0.1337	-0.02966	0.074148
biome stability	-0.31702	0.064799	-0.44414	-0.31707	-0.18976
productivity	-0.16903	0.030591	-0.22907	-0.16904	-0.10899
seasonality	0.24246	0.101583	0.043253	0.242368	0.441993

Phylogenetic beta diversity: Full model.SR (pseudo-R^2 = 0.948)	mean	sd	0.025 quantile	0.5 quantile	0.975 quantile
(Intercept)	12.23145	0.307333	11.62677	12.23186	12.83331
climatic stability	0.120052	0.034258	0.052579	0.120115	0.187114
biome stability	-0.17281	0.041966	-0.25519	-0.17283	-0.09041
topographic heterogeneity	-0.01824	0.013277	-0.04431	-0.01823	0.007805
productivity	-0.09006	0.023282	-0.13584	-0.09005	-0.04443
seasonality	-0.17215	0.071265	-0.31184	-0.17224	-0.03207
log(SR)	-2.74653	0.068963	-2.88166	-2.74663	-2.61099

Phylogenetic beta diversity: Full model – climatic stability.SR	mean	sd	0.025 quantile	0.5 quantile	0.975 quantile
(Intercept)	12.13304	0.308157	11.52698	12.13338	12.73671
biome stability	-0.13794	0.041472	-0.21939	-0.13794	-0.05655
topographic heterogeneity	-0.01314	0.013235	-0.03914	-0.01314	0.012813

productivity	-0.09392	0.023509	-0.14014	-0.0939	-0.04785
seasonality	-0.143	0.071844	-0.28393	-0.14306	-0.00188
log(SR)	-2.72444	0.069149	-2.85998	-2.72451	-2.58858
Phylogenetic beta diversity: Full model – biome stability.SR	mean	sd	0.025 quantile	0.5 quantile	0.975 quantile
(Intercept)	12.36294	0.308163	11.75637	12.36345	12.96619
climatic stability	0.085629	0.033851	0.018967	0.085687	0.151903
topographic heterogeneity	-0.01425	0.013277	-0.04033	-0.01425	0.011784
productivity	-0.12668	0.021748	-0.16939	-0.12668	-0.08402
seasonality	-0.19326	0.072189	-0.33465	-0.1934	-0.05127
log(SR)	-2.77606	0.06915	-2.91149	-2.77618	-2.6401
Phylogenetic beta diversity: Full model – productivity.SR	mean	sd	0.025 quantile	0.5 quantile	0.975 quantile
(Intercept)	12.34498	0.306652	11.74147	12.34545	12.94536
climatic stability	0.125182	0.034315	0.057632	0.125232	0.192386
biome stability	-0.23477	0.03892	-0.31124	-0.23476	-0.15841
topographic heterogeneity	-0.01852	0.013288	-0.04462	-0.01852	0.00754
seasonality	-0.12021	0.0702	-0.25781	-0.1203	0.017784
log(SR)	-2.77202	0.068811	-2.90681	-2.77213	-2.63675
Phylogenetic beta diversity: Full model – seasonality.SR	mean	sd	0.025 quantile	0.5 quantile	0.975 quantile
(Intercept)	12.14176	0.306113	11.53962	12.14212	12.74134
climatic stability	0.110386	0.034289	0.042887	0.110436	0.177542
biome stability	-0.18077	0.042169	-0.26349	-0.18081	-0.09793
topographic heterogeneity	-0.01818	0.013291	-0.04429	-0.01818	0.007883
productivity	-0.07989	0.023012	-0.12516	-0.07986	-0.03482
log(SR)	-2.72639	0.068689	-2.86101	-2.72648	-2.59142
Phylogenetic beta diversity: Full model – topographic heterogeneity.SR	mean	sd	0.025 quantile	0.5 quantile	0.975 quantile
(Intercept)	12.28369	0.304617	11.68449	12.28406	12.88034
climatic stability	0.11455	0.033967	0.04763	0.114618	0.181027
biome stability	-0.16824	0.041766	-0.25021	-0.16826	-0.08622
productivity	-0.09015	0.023263	-0.13589	-0.09013	-0.04456
seasonality	-0.17179	0.071168	-0.31129	-0.17189	-0.0319
log(SR)	-2.75826	0.068353	-2.89222	-2.75835	-2.62395

Table S3. Cape clades sampled for the calculation of phylogenetic diversity and phylogenetic beta diversity metrics of the Cape flora of South Africa. Numbers of species in total, species native to the Cape and Cape endemic species are based on (1).

Clade	Family	No species total	No species Cape	No species endemic	No species included	Data obtained	References
Babiana	Iridaceae	92	60	46	66	Dated tree	2
Bruniaceae	-	79	79	77	53	GenBank sequences	3,4
Cliffortia	Rosaceae	140	125	113	117	GenBank sequences	5
Coryciinae[1]	Orchidaceae	112	44	30	25	Published matrix	6
Disa	Orchidaceae	170	100	82	76	GenBank sequences	7,8
Ehrharta	Poaceae	36	20	12	19	Dated tree	9,10
Erica	Ericaceae	860	680	659	309	GenBank sequences	11
Gladiolus	Iridaceae	250	108	86	94	Dated tree	12,13
Heliophila	Brassicaceae	75	61	38	38	Dated tree	10,15
Lachnaea	Thymelaeaceae	40	40	40	38	GenBank sequences	Direct submission to GenBank, M. van der Bank (U. of Johannesburg)
Metalasia clade[2]	Asteraceae	61	61	54	57	GenBank sequences	15-17
Moraea	Iridaceae	220	122	84	110	Dated tree	2
Muraltia	Polygalaceae	118	109	101	68	Dated tree	9,18
Pelargonium	Geraniaceae	250	150	85	98	Dated tree	9,19
Penaeaceae	-	23	23	23	18	Published matrix	20
Pentameris	Poaceae	83	62	49	58	Dated tree	9, 21
Phyliceae[3]	Rhamnaceae	152	134	127	40	GenBank sequences	22
Podalyrieae[4]	Fabaceae	125	117	109	95	Dated tree	2, 23
Protea	Proteaceae	115	70	65	71	Dated tree	2, 24
Restionaceae	-	545	342	313	261	Dated tree	25
Stilbaceae	-	39	20	17	16	GenBank sequences	26
Total	**-**	**3,585**	**2,527**	**2,210**	**1,727**		

[1] Includes genera *Ceratandra*, *Disperis*, *Evotella*, and *Pterygodium.*
[2] Includes genera *Atrichantha*, *Calotesta*, *Dolichothrix*, *Hydroidea*, *Lachnospermum*, *Metalasia*, and *Phaenocoma*.
[3] Includes genera *Noltea*, *Phylica* and *Trichocephalus*.
[4] Includes genera *Amphithalea*, *Calpurnia*, *Cyclopia*, *Liparia*, *Podalyria*, *Stirtonanthus*, *Virgilia* and *Xiphotheca.*

References for Table S3:

1. Manning JC, Goldblatt P (2012) Plants of the Greater Cape Floristic Region I: The Core Cape flora (South African National Biodiversity Institute, Pretoria). *Strelitzia* 9.
2. Schnitzler J, et al. (2011) Causes of plant diversification in the Cape biodiversity hotspot of South Africa. *Systematic Biology* 60(3):343-357.
3. Quint M & Classen-Bochoff R (2006) Phylogeny of Bruniaceae based on matK and its sequence data. *International Journal of Plant Sciences* 167(1):135-146.
4. Classen-Bockhoff R, Oliver EGH, Hall AV, & Quint M (2011) A new classification of the South African endemic family Bruniaceae based on molecular and morphological data. *Taxon* 60(4):1138-1155.
5. Whitehouse CM (2002) Systematics of the genus *Cliffortia* L. (Rosaceae). PhD (University of Cape Town, Cape Town).

6. Waterman RJ, Pauw A, Barraclough TG, & Savolainen V (2009) Pollinators underestimated: A molecular phylogeny reveals widespread floral convergence in oil-secreting orchids (sub-tribe Coryciinae) of the Cape of South Africa. *Molecular Phylogenetics & Evolution* 51(1):100-110.
7. Bytebier B, Antonelli A, Bellstedt DU, & Linder HP (2010) Estimating the age of fire in the Cape flora of South Africa from an orchid phylogeny. *Proceedings of the Royal Society B* 278: 188-195.
8. Bytebier B, Bellstedt DU, & Linder HP (2007) A molecular phylogeny for the large African orchid genus *Disa*. *Molecular Phylogenetics & Evolution* 43:75-90.
9. Verboom GA, et al. (2009) Origin and diversification of the Greater Cape flora: Ancient species repository, hot-bed of recent radiation, or both? *Molecular Phylogenetics & Evolution* 51:44-53.
10. Verboom GA, Linder HP, & Stock WD (2003) Phylogenetics of the grass genus *Ehrharta*: Evidence for radiation in the summer-arid zone of the South African Cape. *Evolution* 57:1008-1021.
11. Pirie MD, Oliver E, & Bellstedt DU (2011) A densely sampled ITS phylogeny of the Cape flagship genus *Erica* L. suggests numerous shifts in floral macro-morphology. *Molecular Phylogenetics & Evolution* 61:593-601.
12. Valente LM, Manning JC, Goldblatt P, & Vargas P (2012) Did pollination shifts drive diversification in Southern African *Gladiolus*? Evaluating the model of pollinator-driven speciation. *American Naturalist* 180(1):83-98.
13. Valente LM, Savolainen V, Manning JC, Goldblatt P, & Vargas P (2011) Explaining disparities in species richness between Mediterranean floristic regions: a case study in *Gladiolus* (Iridaceae). *Global Ecology and Biogeography* 20(6):881-892.
14. Mummenhoff K, Al-Shehbaz IA, Bakker FT, Linder HP, & Muhlhausen A (2005) Phylogeny, morphological evolution, and speciation of endemic Brassicaceae genera in the Cape Flora of southern Africa. *Annals of the Missouri Botanical Garden* 92(3):400-424.
15. Bengtson A, Anderberg AA, & Karis PO (2011) Phylogeny and generic delimitation of the *Metalasia* clade (Asteraceae-Gnaphalieae). *International Journal of Plant Sciences* 172(8):1067-1075.
16. Bengtson A, Anderberg AA, & Karis PO (2014) Phylogeny and evolution of the South African genus *Metalasia* (Asteraceae-Gnaphalieae) inferred from molecular and morphological data. *Botanical Journal of the Linnean Society* 174(2):173-198.
17. Bengtson A, Nylinder S, Karis PO, & Anderberg AA (2015) Evolution and diversification related to rainfall regimes: diversification patterns in the South African genus *Metalasia* (Asteraceae-Gnaphalieae). *Journal of Biogeography* 42(1):121-131.
18. Forest F, Nanni I, Chase MW, Crane PR, & Hawkins JA (2007) Diversification of a large genus in a continental biodiversity hotspot: Temporal and spatial origin of *Muraltia* (Polygalaceae) in the Cape of South Africa. *Molecular Phylogenetics & Evolution* 43(1):60-74.
19. Bakker FT, Culham A, Hettiarachi P, Touloumenidou T, & Gibby M (2004) Phylogeny of Pelargonium (Geraniaceae) based on DNA sequences from three genomes. *Taxon* 53(1):17-28.
20. Rutschmann F, Eriksson T, Abu Salim K, & Conti E (2007) Assessing calibration uncertainty in molecular dating: The assignment of fossils to alternative calibration points. *Systematic Biology* 56(4):591-608.
21. Galley C & Linder HP (2007) The phylogeny of the *Pentaschistis* clade (Danthonioideae, Poaceae) based on chloroplast DNA, and the evolution and loss of complex characters. *Evolution* 61(4):864-884.
22. Onstein RE, Carter RJ, Xing YW, & Linder HP (2014) Diversification rate shifts in the Cape Floristic Region: The right traits in the right place at the right time. *Perspectives in Plant Ecology Evolution and Systematics* 16(6):331-340.
23. Boatwright JS, et al. (2008) Systematic position of the anomalous genus *Cadia* and the phylogeny of the tribe Podalyrieae (Fabaceae). *Systematic Botany* 33:133-147.
24. Valente LM, et al. (2010) Diversification of the African genus *Protea* (Proteaceae) in the Cape biodiversity hotspot and beyond: equal rates in different biomes. *Evolution* 64(3):745-759.
25. Litsios G, et al. (2014) Effects of a fire response trait on diversification in replicated radiations. *Evolution* 68(2):453-465.
26. Oxelman B, Kornhall P, Olmstead RC, & Bremer B (2005) Further disintegration of Scrophulariaceae. *Taxon* 54(2):411-425.

Fig. S5. Topographic heterogeneity (A) within two minute grid cells and (B) between neighbouring sets (up to eight) of two minute cells (see Materials & Methods). Within cell topographic heterogeneity for the CFR is correlated with between cell topographic heterogeneity (r = 0.632); the former measure was used as a covariate in our spatial regression models.

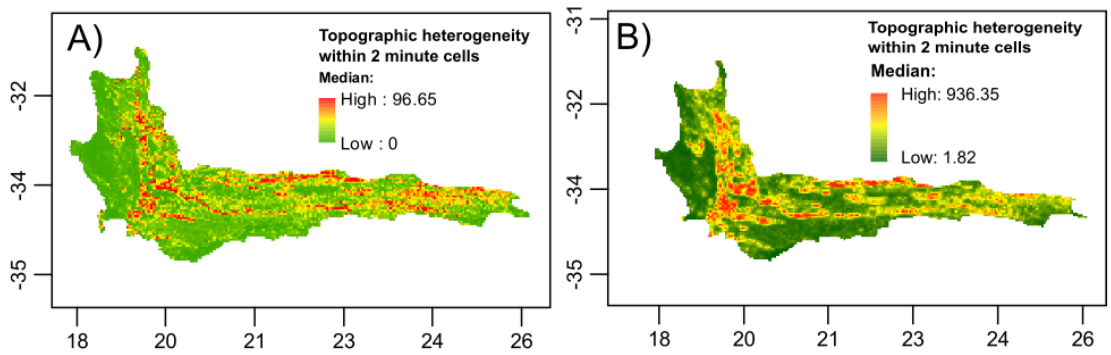

Fig. S6: Bivariate plots of the relationships between the five covariates (all r < 0.6).